THE PHYSICAL CONDITIONS PERTAINING TO SOME POSSIBLE SUPERNOVA REMNANTS

Thesis by

Robert Allan Ridley Parker

In Partial Fulfillment of the Requirements

For the Degree of

Doctor of Philosophy

California Institute of Technology

Pasadena, California

1963

ACKNOWLEDGEMENT

The progress of this research has been aided and also made more interesting and enjoyable by numerous individuals. First, acknowledgement must be given to Dr. Guido Munch who has served as my advisor and Dr. J. B. Oke who has also advised me on many phases but in particular on the use of the scanner for the photoelectric calibrations. Extending this further, virtually all of the members of the astronomy department at Caltech and the members of the staff of the Mt. Wilson and Palomar observatories have also shown me kind interest in the course of this work. Without slighting anyone it seems reasonable, however, to single out a few who have contributed, perhaps, more fully or more frequently. Among this group I must include Drs. Minkowski, Greenstein, Schmidt, Wilson, Sargent, Hodge, Wildey, and O'Dell. In true Academy Award fashion but actually for real service rendered I must also mention Messers Blackee, Hancock, Kearns, Miller, Olmstead, and Ratzlaff, and Miss Swope.

Acknowledgement must also be made of those who have financially supported me during my four years of graduate study and research, Caltech, the Danforth Foundation, the National Science Foundation, the Woodrow Wilson Foundation, and my wife, Joan. To her, of course, is due far more than merely credit for financial support and as a sign of the innumerable indefinable credits due her,

I affectionately and appreciatively dedicate this thesis to her.

ABSTRACT

A large number of spectrophotometric observations have been made of 16 individual filaments in five possible supernova remnants, S 22, S 147, IC 443, NGC 6888, and the Cygnus Loop. Using these observations and making certain assumptions regarding abundances (that relative to Hydrogen we will expect abundances to be at least normal), it is shown that temperatures vary greatly within the filaments but are generally of the order of ten to fifteen thousand degrees for the regions from which we receive most of the [OII], [NII], [SII], and Balmer emission. The densities for these same regions are of the order of a few hundred electrons per cubic centimeter. From these conclusions it is further indicated that: 1) the source of excitation of the Balmer lines is collisional; 2) all of the observed radio radiation from IC 443 and the Cygnus Loop can, by extrapolation from the observed total H_α flux, be accounted for as thermal radiation; 3) the total mass of the visible filaments of IC 443, NGC 6888 and the Cygnus Loop is of the order of several tens of solar masses; and 4) the apparent filaments are actually only the results of the projection effect for shells.

INTRODUCTION

Within the general classification of galactic emission nebulae there is a small sub-group of objects exhibiting to a greater or lesser degree sharp filamentary structure. Slightly more than a dozen of these nebulae have been catalogued cf. Harris (1961) and virtually all of them have been found to have a nominally nonthermal spectrum in the radio frequency region. Three of the members of the sub-group are associated with the three well-known supernovae of the galaxy, and for this reason as well as for reasons pertaining to our ideas about the sizes of these objects and the energies involved in them, it is generally admitted that these filamentary nebulae are the remnants of supernovae.

Although the limitations of time have prevented astronomers from obtaining any direct astrophysical observations regarding the evolution and origin of these objects, a certain amount of useful information that may indirectly bear on these aspects can be gleaned from proper spectrophotometric observations of the supposed supernovae remnants in their present state.

Since the physical conditions within a gaseous nebula govern the relative intensities of the spectral lines that are observed in emission, if an understanding can be obtained of the processes behind the emission of the radiation, then calculations can be made which will predict for various physical conditions the relative intensities that would be observed. Comparison then of the relative intensities of the various lines as emitted by a particular nebula with the predicted

relative intensities will allow us to choose the set of physical conditions that probably exist within the nebula. Such an understanding of the processes of emission does indeed exist and can be exploited for several lines including, for instance, the Balmer lines, the [NII] doublet, at λ6548 and λ6583, the [OII] doublet at λ3726 and λ3729, the [OIII] doublet at λ5007 and λ4959, and the [SII] doublet at λ6716 and λ6731. Consider first the forbidden lines. Since the ground configuration of the ions involved is comprised of three close lying states, calculations can be made treating the various ions as 3 level atoms for which we can rather easily write down equations relating the populations of the individual levels in terms of detailed balancing between the number of transitions into and out of a given level. In this way for a particular stage of ionization, the number of ions in a particular state can be computed. Cross-sections and transition probabilities of varying quality are available in the literature. Since each of the forbidden doublets discussed above comes from a different element or stage of ionization, these computations do not directly aid us in calculation of the relative intensities of the doublets to one another. It should be noted that there does exist for the OIII ion another forbidden line at λ4263 which arises from the third level. (The two lines listed above arise from the second level.) The ratio of the intensity of the line at λ4363 to the intensity of the doublet would thus give a direct measure of the temperature. The difficulty that arises here is that being only 5 A from the Mercury line at λ4358 the [OIII] line is completely overpowered by the Mercury line arising from the reflection of the Los Angeles lights. Likewise there are other lines for the NII, OII, and SII ions which arise

from the third level and could give direct values of the temperature with depending on ionization or abundance but which are either inconveniently located or too faint or both and so were not included in the present study.

Using the Boltzmann-Saha equation, as corrected for departures from Thermodynamic equilibrium, calculations can be made of the population of the various levels for the Hydrogen atom. The calculation of the corrections is dependent on the temperature, and other physical circumstances such as whether or not the nebula is optically thick to Lyman radiation, what the source of the excitation is and what the shape of the ultraviolet tail of the radiation field is. Calculations of the corrections are available in the literature for some cases. One of the main factors to which the population of the levels of the Hydrogen atom is sensitive is the source of excitation. The actual details of this dependence will of course be dependent on the cross-sections for radiative and collisional excitation and ionization. In a rough manner it can be said that for the collisional case as opposed to the radiative case there will be relatively more atoms in the third level compared to the fourth level. Hence the ratio of $I(H_\alpha)/I(H_\beta)$ will be larger for the collisional case relative to the radiative case, and the measurement of this ratio will allow us to discriminate between the two modes of excitation.

The question of the source of excitation for these nebulae is important because of the fact that no exciting star is known to be associated with them. The case of radiative excitation is still possible since the high energy tail of a non-thermal continuum could possibly give rise to the excitation, as is the case with the synchrotron radiation of the Crab

Nebula. On the other hand, Oort (1946) has proposed that the source of excitation may lie in the interaction of the expanding shell with the interstellar medium. In the same way, more detailed discussions have also been put forward e. g. Sargent (1959) considering the form of the interaction as a shock wave which among other things introduces stratification with a relatively less dense extremely hot region, immediately behind the shock, that cools and condenses.

For two of the ions, OII and SII the doublets at λ3727 and λ6725 are formed by transitions from two different upper levels to a common lower level. Since the transition probabilities for radiative deexcitation from the different upper levels and also the collision strengths for excitation from the ground level to the different upper levels are not identical, the relative intensities of the two lines of the doublet are functions of the density. Therefore observations of the doublet ratio for the two doublets, [OII] and [SII], can indicate the density that exists where these lines are formed.

As far as the ratios between the doublets are concerned, if the degree of ionization is known, and if the elemental abundances are known, then it will be possible to compare the number of ions for one element in a particular state of a particular stage of ionization with the corresponding number for another element, and thus predict the relative intensities of the lines. Generally for gaseous nebulae the computation of the degree of ionization is complicated by the need to know the dilution factor and the shape of the ultraviolet tail of the stellar radiation that is doing the exciting and ionizing. For the case where there is no radiation field the problem of ionization becomes somewhat simpler since the ionizing is done by the same electrons which excite the for-

bidden lines and whose temperature we shall hope to be able to determine. Complications arise, however, in connection with the cross-sections for the collisional ionizations. No good ones have been determined and in the present paper recourse is had to the method of equating the number of photorecombinations with the number of collisional ionizations and comparing the ions concerned to the Hydrogenic case. The two ions of Oxygen for which we have forbidden doublets offer a possibility of indicating the degree of ionization without being bothered by the question of elemental abundances. However, we should notice that if any stratification or inhomogeniety occurs then there is every reason to expect the [OIII] radiation to come from the hotter regions and the [OII] radiation to come from the relatively cooler regions. All of the other emission lines being discussed, including the Balmer lines but not the [OIII] lines, will in the case of varying temperatures be formed in regions of more or less similar temperatures and so if elemental abundances are known an average temperature can be obtained more or less independent of stratification, from the observed relative intensities.

The question of abundances is a bit hard to answer, however. If the objects concerned here are the remnants of supernovae, then according to present ideas of nucleogenesis large quantities of non-Hydrogenic elements ought to have been expelled by the supernova. These overabundances will be diluted by interaction with the interstellar matter originally present in the volume now enclosed by the remnant. It is not obvious, however, that this effect will reduce the overabundances to nil since an overabundance of 1000 or more in a solar mass of material

diluted by 100 solar masses of interstellar material will still result in an overabundance of a factor of 10 for the whole mass. One point is clear as to what we will expect for abundances; they should not be less than the original abundance of the interstellar matter. A shell of pure Hydrogen thrown off by the supernova would have negligible diluting power unless it were large compared to the mass of interstellar matter originally present in the volume -- a condition that presently seems unlikely.

From the calculations discussed above, one other attack can be made that is not directly connected with spectrophotometry. Since the calculations for Hydrogen indicate the "efficiency" of an individual Hydrogen atom or ion in producing H_α radiation as a function of temperature and density, if the total flux, at the earth, in H_α from an object, and its distance are known, then the total number of Hydrogen atoms and ions in the visible portions of that object are also known and hence the mass. Going in the other direction, once we have the total number of hydrogen atoms and the distance of the source we can also compute the expected free-free emission in the radio region.

Attacking the same problem previously mentioned in connection with the Balmer decrement it is of interest to know how much of the radio emission is due to non-thermal causes and thus how much energy is available in the high energy tail of the synchrotron radiation. If it can be shown that there is not enough energy available from this source to balance the energy losses of the nebulae then we have an independent check on the conclusion that the source of excitation must be collisional.

One aspect of the problem that has been allowed to pass without comment so far is the influence of interstellar absorption and reddening on the line intensities as observed at the earth. For these objects with whom no stars are known to be associated, the reddening in that direction cannot be determined by simply measuring the reddening of the exciting stars. By observing many stars in the direction of the object both in front of and beyond the object, the run of absorption with distance can be determined. Therefore if the distance to the object is known the absorption in front of it is determined.

The determination of the distance to these remnants is basically very simple. We can measure a radial velocity of expansion and compare it with the proper motion of expansion. In practice, however, because of the large size and faintness of the objects, only one distance determination has been made on this basis. Even for this procedure there is some uncertainty since the motion of the individual filaments may actually be comparable with the general motion of expansion.

In the present work we will consider only a few of these objects listed by Harris (1961) including S 22, S 147, IC 443, NGC 6888, and NGC 6960, 6992 and 6995 (the Cygnus Loop). Our selection is based primarily on the feasability of obtaining good observations with the instruments and time available.

S 22 (1-27-28, +58-06:1950) is a small, 10 x 11', example which appears primarily as an elbow. S 147 (5-36, +28:1950) is the largest example considered here, as much as four degrees in diameter. It is very faint and filamentary in appearance, having many delicate loops,

although the filaments are not in general particularly sharp.

IC 443 (6-14-16, +22-36:1950) is extremely similar in appearance to the Cygnus Loop, with a great many very sharp filaments near the edges and some more diffuse patches of emission in the middle. It is about one degree in diameter or one third of the size of the Loop. From the appearance of the star field in which it is imbedded it is obvious that there is very patchy obscuration in that direction; it is very close to the plane of the Milky Way.

NGC 6888 (20-10-55, +38-15:1950) is a small example, 11 x 16'. Hubble (1922) has suggested that it may be the remnant of a nova outburst. It is not extremely filamentary in appearance and may be associated with the Wolf Rayet Star HD 192163. It is certainly a very unusual appearing ring-shaped nebulosity. It is right in the plane of the galaxy and is probably heavily obscured.

The Cygnus Loop (20-50, +30-30:1950) is by far the best known example of this sub-group. It is about three degrees in diameter. Lying about nine degrees off the galactic plane it is probably obscured although not too heavily. Certainly the obscuration, from the appearance of the star field, is fairly uniform. Like IC 443 it is not really a complete ring but still appears more or less to be composed of portions of a circumference with the interior regions relatively free of emission nebulosity.

HISTORICAL BACKGROUND

The first work on the Cygnus Loop was a part of Hubble's investigation of the distinctions between reflection and emission nebulae (Hubble 1922). At that time he concluded that he could find no exciting star for the loop even though it was of the emission type. Several searches by others since then e.g. Balonowsky and Hase (1935) and Miller (1937) also failed to find an exciting star for the Cygnus Loop. Hubble (1937) measured the rate of expansion of the Cygnus Loop, from plates taken at a 27 year interval, as $0.''03$ per year. From measures of the radial velocities of many locations in the Cygnus Loop, Minkowski (1958) derived a picture of the Loop as a thick shell whose outer edge is expanding with a velocity of 116 km/sec and thus using Hubble's measures obtained a distance of 770 parsecs. A few spectrophotometric observations have been made by Code (unpublished) and Osterbrock (1958) to determine the temperature and density of some of the filaments in the Cygnus Loop; from their work temperatures of the order of 40,000 ^{o}K and mean densities of 200 electrons per cm^3 are indicated. Similar observations have also been made to measure the ratio, H_α/H_β, for the Cygnus Loop since the Balmer decrement is dependent on the type of excitation, collisional or radiative (Chamberlain 1953). The results of observations by Chamberlain, Humason, Pickelner, and Minkowski have been summarized and discussed by Minkowski (1958). At that time a Balmer decrement, $I(H_\alpha)/I(H_\beta)$, of 3.4 was adopted and taken as indicating collisional excitation. Two points must be noted about these results, however. First, the figures used are mean values which do

not always include the same points and thus may be misleading in view of the rather large variations in relative intensities of various spectral lines from filament to filament. Second, no apparent correction has been made for reddening which may have a rather large effect on such ratios as H_α/H_β, and 3726+3729[OII]/ 5007+4959[OIII]. Except for two observations of the density of one filament in IC 443 and an estimate of the proper motion of expansion of IC 443, no other detailed observations of the objects to be considered here are known, at least in published form.

PROGRAM

The possibilities for further study are obvious. Most important would seem to be a detailed spectrophotometric study of several individual filaments. Such a study, using both spectrographic plates of different spectral regions and photoelectric spectral scans to connect the various spectral regions, should allow us to obtain line ratios, including the Balmer decrement, which in conjunction with the proper calculations will indicate the physical conditions of temperature, density, and abundance that exist in the filaments and also indicate whether the excitation of the Balmer lines is due to an ultraviolet radiation field or inelastic collisions between Hydrogen atoms and electrons. Obviously we should also like to know the effect of interstellar absorption and reddening on the observed relative intensities of the spectral lines. Third, a study of the velocity of expansion of the various objects would increase our understanding of their dynamics, and form. In the same manner any further information that could be found concerning the proper motion of expansion of the objects under discussion would be of interest. Finally if measures could be made of the total monochromatic flux from these objects, they would allow us to investigate, among other things, the mass of the visible filaments, their total requirements for energy input in order to maintain equilibrium, and a means of comparing optical and radio observations. This in brief is the program that was carried out to a greater or lesser degree in observing the objects listed earlier.

INSTRUMENTATION

The spectrograms of the individual filaments were obtained using the Mt. Wilson Newtonian Focus Spectrograph. The grating 83A which is blazed for approximately λ6500 in the third order, λ4900 in the fourth order, and λ3900 in the fifth order was used. With the f/0.5, 1.5 inch focal length solid Schmidt camera we obtain approximately 240, 180, and 144 Å/mm on the plates for third, fourth, and fifth orders respectively. There is also an f/1.0, three inch focal length camera which was used in the ultraviolet and which when used with grating 83A yields about 67 Å/mm in the fifth order. Although designed for a three inch beam the spectrograph uses an f/5, ten inch colimator and therefore has a scale factor of 1/6.7 for the solid Schmidt and 1/3.3 for the three inch camera. A slit width of 0.11 mm was used for exposures with the solid Schmidt and a width of 0.07 mm was used with the three inch camera. This results in a projected slit width of 15 and 22 microns respectively.

Photoelectric scans were made with the Mt. Wilson cassegrain scanner operating at the 100" cassegrain. This scanner has previously been described by Oke (1960). Dispersion at the exit slit is 20A/mm in the first order and 10A/mm in the second order. The grating is blazed for about λ3500 in the second order. For observations in the second order longward of λ4700 a K2 filter is used to eliminate the third order ultraviolet. For work connecting the ultraviolet and green spectral regions a 1P21 photocell was used, while for work connecting the red and green regions a red sensitive RCA 7237 photocell was used.

It should be noted that since the scanner is not equipped for off-setting the positioning of the slit on the regions of interest is the weakest part of the observing procedure. The slit has to be set by eye with respect to field stars which were on occasion very few and faint. Once the slit had been set, however, it was possible to guide on a general field star and thus keep the slit rather stationary.

OBSERVATIONS

Filaments were picked in most cases on the basis of sharpness and to a certain extent their position. In a few cases in the Cygnus Loop they were picked with regard to their color. Actually a great many filaments were at first picked in IC 443 and the Cygnus Loop and these were then rather arbitrarily weeded out. Figures 1 and 2 are the finding charts for all the filaments studied. The position of the scanner slit along the spectrograph slit is indicated by the arrows. The numbers following the designation of the objects specify the location. The slit location for the scanner is specified by a plain number e.g. in IC 443-6 whereas the slit location for the spectrograph is specified by n' e.g. IC 443-6' which is associated with the scanner location, IC 443-6 but is obviously not identical with it. Certain exceptions were forced on this system by changes in the program. Thus IC 443-66 and IC 443-6" are associated; IC 443-77 and IC 443-7' are associated; and NGC 6960-8 and NGC 6960-88 are both associated with NGC 6960-8'. (NGC 6960-8 is the lower location.) Lettered stars are BD stars and are listed in Table 1. When more than one BD star is present on a finding chart only one is still indicated. North is always at the top and east at the left.

For S 22 one slit position suffices to cover both filaments and the interfilamentary region. Since the filaments are rather thick, their widths projected perpendicular to the dispersion on the plates is not prohibitively small. The slit is left EW as a matter of simplicity. For S 147 only one filament was judged sufficiently sharp and bright to

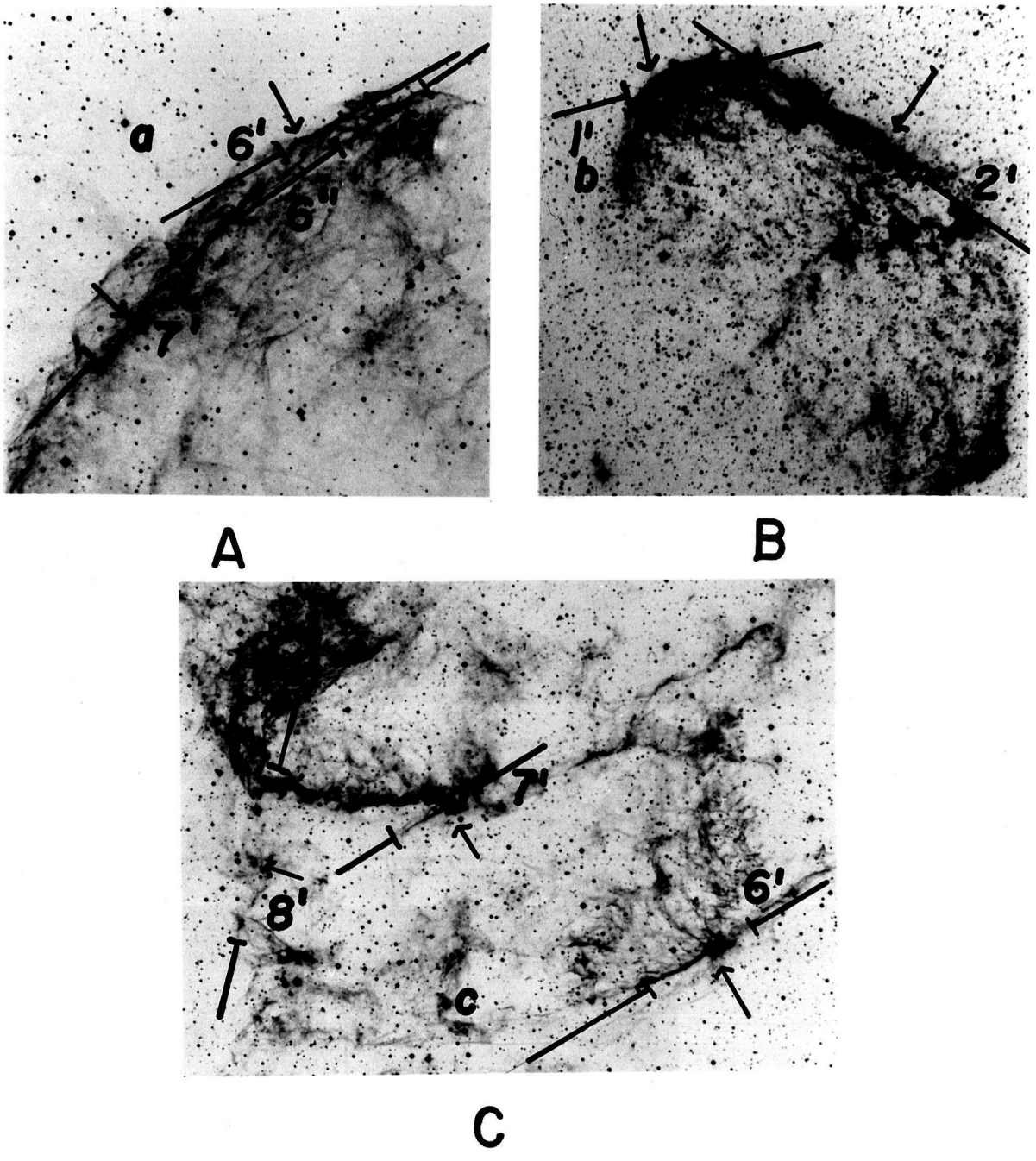

Figure 1: A - IC 443-6', -6", -7'.
B - NGC 6888-1', -2'.
C - NGC 6960-6', -7', -8'.

Scale: 13"/mm.
Oriertation: North at top; East at left.

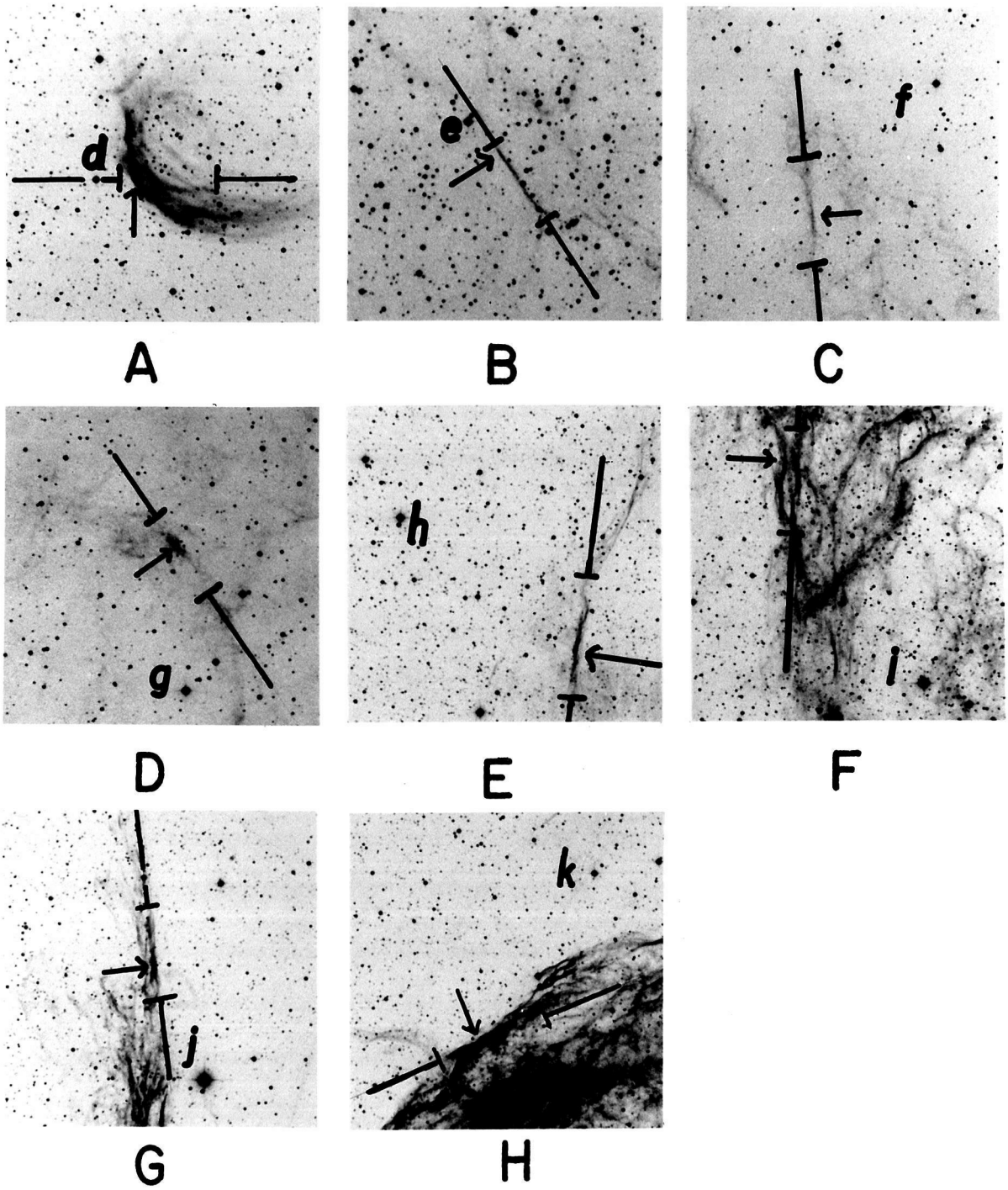

Figure 2:

A - S 22-1'.
B - S 147-1'.
C - IC 443-15'.
D - IC 443-16'.
E - NGC 6960-2'.
F - NGC 6960-3'.
G - NGC 6960-4'.
H - NGC 6960-12'.

Scale: 13"/mm.
Orientation: North at top; East at left.

TABLE 1

BD STARS ON FINDING CHARTS

Letter	Star
a	+ 22°-1268
b	+ 37°-3827
c	+ 30°-4245
d	+ 57°-305
e	+ 28°-872
f	+ 22°-1247
g	+ 22°-1249
h	+ 30°-4194
i	+ 30°-4184
j	+ 30°-4166
k	+ 31°-4269

be of particular interest. For IC 443 the first three filaments are all in the N. E. quadrant and are at or very near the edge. The second two are in the N. W. and the S. W. portions respectively, and are further from the edge, especially number 16. Virtually all of NGC 6888 is included in the finding chart. The two slit positions do not lie along any particular filaments, which are for this object quite irregular and broken, but just include the two brightest portions of the rim. For the Cygnus Loop positions 2 and 3 are located in the long system of filaments located to the West of the center but separated from the western edge, and are therefore relatively far from the edges, especially number 2. Number 4 is located near the top of the western edge. Numbers 6, 7 and 8 are located in NGC 6995. These three, especially number 8, were picked to study this rather unusual appearing area. Number 12 is located at the edge near the top of NGC 6992.

Spectrographic observations were attempted on a total of 70 nights from December 1960 to March 1962. For most of the filaments studied this resulted in two plates in each of the three spectral regions. During exposures the filaments were kept stationary on the slit and thus the spectral lines on the plates are not uniform but indicate the appearance of the filament on the slit. To calibrate the plates for intensity, plates were also run in the 60" (or 100") wedge spectrograph. As is customary, exposure times for the latter plates were set to within a factor of two of that for the plates taken at the telescope and both plates were taken from the same box and processed together. For the red exposures, 103_aF plates were used with the solid Schmidt camera together with an

OG filter which cuts off sharply at λ5500, eliminating the fourth and fifth orders. For the green exposures baked II_aO plates were used with the solid Schmidt camera together with a Wratten 2A gelatin filter which cuts off short of λ4300 and eliminates the fifth order. For the ultraviolet plates we again used baked II_aO plates but this time with the three inch camera together with a Corning 5970 filter which cuts off longward of λ4100 until it reaches the red.

With the red plates we observed the [SII] lines at λ6716 and λ6731, the [NII] lines at λ6583 and λ6548, H_α, and the [OI] lines at λ6364 and λ6300. The latter were observed primarily in IC 443 and as far as could be told were always contaminated with night sky emission, hence their intensities were not reduced and considered quantitatively. Virtually no continuum was ever observed on these plates. With the green plates we observed the [OIII] lines λ5007 and λ4959, H_β, and the Mercury line λ4358, sometimes accompanied by H_γ but these last two were just at the edge of the focus and H_γ was too much on the wings of the Mercury line to be of any use. The [OIII] line at λ4363 was much too close to the Mercury line to be seen. Varying amounts of continuum were observed on these plates, but it was never possible to critically determine whether this was due to reflected valley lights, or a real continuum from the filament. At times it was also probably helped by moonlight although virtually all the plates were taken during dark time. On at least one occasion it was also helped by scattered starlight from a bright star just off the slit. It can be said that at no time was it demonstrated that the variation of the intensity of

the continuum along the slit mimicked that of the emission lines or filament. The main lines of interest on the ultraviolet plates were the [OII] lines at λ3729 and λ3726. Using the three inch camera with a dispersion of approximately 67 Å/mm it is possible to resolve the doublet and thus measure the ratio of the two components. Also observed on some of the plates was the [NeIII] line at λ3869. Virtually no continuum was ever observed on these plates.

For the purpose of obtaining the sensitivity function of the plate-instrument combination as a function of wavelength, exposures were also made, with the same instrumental setup, of two standard stars, HD 15318, a B_9 III star, and HD 130109, an A_0 V star, whose energy distributions are known from spectral scans. Although there is a large difference in the exposure times between these plates and the nebular plates the comparison of wavelength sensitivity should be valid since both sets of plates had their own appropriately exposed wedges. For this program of calibration, a set of plates, generally consisting of two exposures for each spectral region, was usually obtained each run.

Useful scanner observations were obtained on seven nights in 1961, and on two nights in 1962. The general procedure in using the scanner was to observe the intensity of one line in the red and one line in the green with the red cell on one night, and observe the same line in the green and one line in the ultraviolet with the blue cell on another night. For most filaments only one set of observations comparing the green and red and one set comparing the green and ultraviolet were obtained.

It was found that in order to get reasonable signals above the level of the dark noise it was necessary to use the scanner as a current integrator with an entrance slit of 2 x 4 mm. This is also roughly equal to the size of the brightest parts of many of the filaments which were studied. The two mm width was in the east-west direction and necessitated the use of at least two mm exit slit, corresponding to 20A and 40A in the second and first orders respectively. In practice 30A and 50A exit slits were used to allow for possible error in the centering of the band on the wavelength in which we were interested. The resulting sensitivity function for the band pass for a uniformly filled entrance slit at a particular wavelength is a trapezoid whose shorter base is 10A and whose longer base is 50A or 90A for the second or first order respectively. The procedure was to take one measure on the continuum longward of the line where no night sky or nebular lines were known to exist, then one on the line, then one on the shortward continuum, then repeat the line, then through the same procedure for the other spectral region, then back and repeat the cycle. The two cycles yield what we refer to as a set of integrations.

Integrations were made in the red at λλ6632, 6562, and 6454. The second position centered on H_α includes also the [NII] lines. Corrections for this were later made on the basis of the observed relative intensities of each of the [NII] lines and H_α and the sensitivity function described earlier. These observations were carried out using the first order. Integrations were made in the green at λλ5051 (5040), 5007, 4911 (4925), and sometimes λλ4861 and 4811 (4825), depending on

whether observations were being made in the first or (second) order. Observations were made in the first order when comparison was being made with the red and in the second order when comparison was being made with the ultraviolet. Integrations in the ultraviolet were made at λλ3760, 3727, and 3694. These measures were made using the second order. Since these filaments have virtually no continuum, the readings on the continuum actually represent sky readings. Readings were made on occasion on the sky nearby a few of the filaments and no real difference between continuum and true sky readings could be found.

Calibration of these measures was obtained by taking a few scans each night of standard stars. The stars used were HD 15318, HD 130109, and HD 172167 (α Lyrae). All measures are referred to the intensity of α Lyrae at λ5560 which is taken as unity and measured absolutely as 3.8×10^{-9} ergs/cm^2/sec/A. To connect the integrations of the filaments and the scans of the standard stars, a few of the brightest filaments were also scanned, and then artificial gains introduced in reducing the integrations to force integrations and scans for the filament to agree. These gains were then adopted for the other observations as well.

In order to determine the amount of interstellar absorption in the direction of the Cygnus Loop, a series of UBV measures were made. Paul Hodge kindly consented to make some of these. The author made measures of 8 standards and 32 unknowns on two nights in June of 1962. The stars used for this purpose were picked by blinking the sky survey plates which included the loop, taking stars of approximately the 12th

magnitude which appeared blue.

In order to try to measure the proper motion of expansion of IC 443 a second epoch plate was taken attempting to duplicate H 1036 B, taken by Baade in 1939. Although the plate was usable the observing conditions and hence the quality of the plate were not as good as those for the first epoch plate. C. R. O'Dell was kind enough to obtain this plate.

With an eye towards measuring the total monochromatic flux from the objects under discussion, a series of plates was taken of all the objects with the 48" Schmidt using 103aE's and an OR-1 filter, which combination passes primarily the [NII] lines and H_α, there being a strong cutoff at λ6300 and λ6650.

REDUCTION

The UBV measures of the stars in the direction of the Cygnus Loop were reduced using a program written by Abell for the IBM 7090. The intrinsic colors of the stars were then determined by assuming that the stars all belonged to luminosity class V and using the two color diagram and reddening lines. Since spectral classes were not known for the stars a certain ambiguity arose at this point since many of the stars could be followed back on the reddening lines to either one or two points on the two color relation. For these stars therefore two solutions were carried out in the work that followed. Using the relation developed by Wildey (1962) between monochromatic interstellar absorption, and color excess and intrinsic color, the amount of absorption, represented by the parameter, $\rho\ell$, was determined for each star. The actual monochromatic absorption in magnitudes is obtained by multiplying the values listed by Oke (1961) by $\rho\ell$, i.e. a value of E(B-V) of + 0.14 corresponds to a value of $\rho\ell$ of 1.0. The true distance of the stars was calculated by taking the visual absorption equal to 3E(B-V) and by using absolute magnitudes from the MK system (Keenan and Morgan 1951) after determining MK spectral classes from Johnson and Morgan (1953). The resultant relation between the absorption parameter $\rho\ell$, and distance is plotted in figure 3. Filled circles represent stars for which no ambiguity is apparent. Open circles are from the redder solutions of stars for which there is an ambiguity and the open squares are from the blue solutions of the same stars. The line is a somewhat weighted visual estimate of the mean and indicates a value of $\rho\ell$ of 1.3 at the

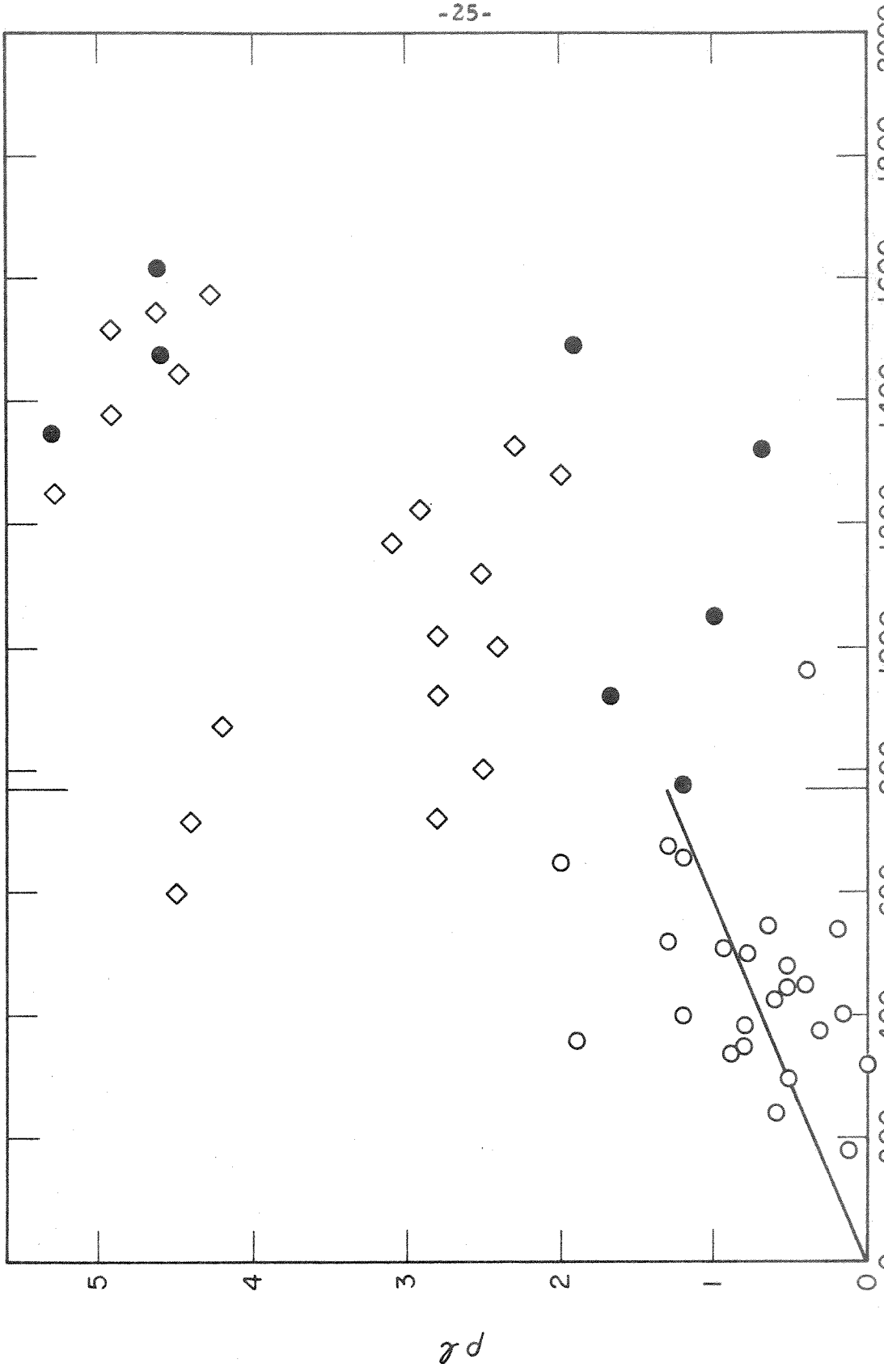

Figure 3: The parameter ρl as a function of distance in the direction of the Cygnus Loop.

distance of the Cygnus Loop. Since the two different solutions for a star tend to lie along the mean line, i.e. the bluer solution will indicate more absorption but will also indicate that the star is further away, we may expect that this mean line through all the points will be not too far from the truth. To test the dependency of the line on the actual distribution of the stars as either blue or red solutions, ambiguous stars were assigned on the basis of the flip of a coin to one or the other solution for five different sets which were also reversed giving us two series of five sets of random distributions among the spectral types. Lines were then drawn through each plot; the resultant average value of $\rho\ell$ at the Cygnus Loop was 1.23 with a maximum spread of 0.17. This corresponds to a value of +0.17 for E(B-V) with a maximum spread of 0.02, and an uncertainty in the reddening correction for the intensities of the nebular lines of 2% for the correction between red and green or green and ultraviolet, and 5% for the correction between red and ultraviolet.

Hiltner (1956) lists observations of 4 B stars in the approximate direction of NGC 6888. The values of $\rho\ell$ determined from his measures scatter a bit but average to about 3.8. Miss Roman (1951) has also studied this general region including two of the stars measured by Hiltner and also by indirect methods the Wolf Rayet star at the center of NGC 6888. Her measures lead to a value of $\rho\ell$ of 3.6 and therefore a mean of $\rho\ell = 3.7$ was adopted. Three stars in the direction of IC 443 have also been measured by Hiltner (1956) and these lead to values of $\rho\ell$ varying from 4.6 to 7.9. It was not felt safe to use these values directly since

as mentioned earlier the obscuration is obviously very patchy in that direction. They were however used as rough checks on the values determined for the individual filaments on the basis of assumed constant abundances as described elsewhere.

A source of unknown systematic error particularly for NGC 6888 and IC 443 lies in the fact that the distances to these objects are not well known. There are, however, other indirect limits on the reddening that we can discuss in the conclusion and which will indicate that the values for the reddening for IC 443 and NGC 6888 as indicated above are approximately correct.

All of the observations made with the scanner were reduced through the use of a program developed by Oke for the Burroughs 220 computer. For the scans of the comparison stars the continuum was drawn in and the deflection, proportional to intensity, was measured for the wavelength of each of the nebular lines of interest as well as those points where integrations of the continuum were made with the scanner in observing the filaments. The absolute energy distributions obtained in this way were then also used, in connection with the energy distribution derived from the stellar spectrograms, to obtain the wavelength sensitivity of the various plate filter combinations. The absolute energy distributions obtained for HD 15318 and HD 130109 are listed in Table 11 of the Appendix page 107.

Since the nebular observations with the scanner consisted of integrations on and off the positions of the emission lines the reduction procedure was slightly different. The result of this work was to yield a

series of measures arising from the continuum readings proportional to the intensity of the sky plus the dark current and a series of measures arising from the emission line readings proportional to the intensity of the filamentary emission line plus the sky plus the dark current. Thus the continuum values were first corrected by a factor equal to the difference between the instrumental sensitivity function at the continuum wavelength and the wavelength of the emission line concerned. Once this had been done for the continuum on both sides of an emission line, the two values would be averaged and the result subtracted from the intensity of the line plus sky plus dark current. The uncertainty of an individual measure is rather large, especially for the fainter filaments since the dark current on some runs accounted for 80 or 90% of the total signal even for average filaments. This net value was fed into the computer which yielded the true observed intensity in magnitudes, from which we then subtracted the instrumental sensitivity function (OB-AB), as derived from standard stars, to obtain an absolute value for the intensity of the emission lines. The intensities in magnitudes measured in this fashion are listed in Table 2. The values given are relative to the intensity of α Lyrae at $\lambda 5560$ which is set as $0^m.00$ in the system -- the actual intensity of that point being taken absolutely as 3.8×10^{-9} ergs/cm^2/sec/A -- and are averages of 4 to 6 measures so that some of the uncertainty discussed above has been removed.

It should be noted that in Table 2 a measure of about 14^m with the red cell corresponds to a minimal difference between the continuum and the line (in fact this value was also used in the data fed into the computer

TABLE 2

INTEGRATIONS (MAGNITUDES)

Object	Date	λ6562	λ5007	λ4861	λ3727
S 22-1	1-8/9		13.66		12.87
	10-10/11	10.33			
	10-10/11	10.32			
	10-11/12	10.13	(12.71)		
	1-7/8	9.80	(12.07)	(12.08)	
S 147-1	1-8/9		13.34	13.96	12.65
	10-11/12	12.24			
	1-7/8	(11.77)	(12.19)		
IC 443-6	1-8/9		12.47	13.31	12.43
	10-10/11	9.70	11.88	~12.1	
	1-7/8	9.66	11.63		
IC 443-66	1-8/9		11.66	13.12	11.81
	1-7/8	9.75	11.42		
IC 443-77	1-8/9		13.95	13.31	13.04
	1-7/8	9.82		(11.77)	
IC 443-15	1-8/9		(13.75)	(14.96)	(13.90)
	1-7/8	11.59			
IC 443-16	1-8/9		13.53	13.53	12.87
	1-7/8	10.17			
NGC 6888-1	7-7/8		11.65	11.51	12.41
	7-8/9	7.99	11.45		
NGC 6888-2	7-7/8		10.14	11.41	12.98
	7-8/9	8.46	10.08	10.91	
NGC 6960-2	8-11/12		12.04		11.63
	7-9/10	9.81	11.12		
	10-10/11	10.17	11.17		
NGC 6960-3	8-11/12		11.47		10.35
	8-11/12				10.29*
	7-9/10	9.71	11.04		
	10-10/11	9.61	(10.71)		

TABLE 2 (Continued)

Object	Date	λ6562	λ5007	λ4861	λ3727
NGC 6960-4	7-7/8		9.89	12.40	10.06
	7-8/9	9.79	10.15		
NGC 6960-6	8-11/12		10.68		9.80
	8-11/12				9.75*
	7-9/10	8.86	11.06		
NGC 6960-7	7-7/8		10.86	11.25	9.34
	7-8/9	8.60	10.48	(11.26)	
NGC 6960-8	8-11/12		9.55		10.69
	7-8/9	10.79	9.55		
NGC 6960-88	10-10/11	9.80	10.96		
NGC 6960-12	8-11/12		11.52		10.67
	7-9/10	9.28	10.88		
	10-10/11	9.30	11.41		

Remarks:

1) Values enclosed in parentheses are of lower quality.
2) * sign indicates values obtained by scanning to calibrate integration system.
3) Magnitudes are relative to the intensity of α Lyrae at λ5560 for a 5 Å band pass.

for all cases where the difference was negative or zero). With the 1P21 the sensitivity is about 3 magnitudes better. To obtain a value for the intensity of H_α from the figure for the intensity measured at $\lambda 6562$ we must know the contribution from the [NII] lines. The relative strengths of the lines vary from filament to filament but can be determined from the nebular spectrograms. From our knowledge of the sensitivity function of the band pass as determined by the entrance and exit slits of the scanner we find that

$$I(6562) = I(H_\alpha) + 0.58\, I(6584) + 0.78\, I(6548).$$

In the same fashion we determine the intensity of $\lambda 3726$ from our measures of I(3727) by measuring the ratio of $\lambda 3729$ to $\lambda 3726$ and setting the sum of the two lines equal to I(3727). It can be easily noticed from Table 2 that the values of I(5007) do not always agree with each other for the same filament as measured on different nights with different cells. For filaments that were measured on different nights with the same cell the same effect can also be noticed. The cause of this scatter is very probably the difficulty, mentioned earlier, in setting the slit of the scanner in the exact location. In collecting these values for a single filament the discrepancy was removed by setting the values of I(5007) equal to the brightest value observed and then adjusting the I(6562) or I(3727) connected with the fainter value accordingly. This procedure is not altogether arbitrary and prejudiced toward yielding values of I that are too bright since it can be argued that after all the instance in which we observed the filament at its

brightest must be the time that we came closest to setting correctly on it.

At this point it would seem appropriate to say something about the quality of the observed measures of the individual filaments. For S 147 the tie in between the red and green integrations is poor. For IC 443-6 and -66 the tie in is good but a problem arises in that the $H_\beta/\lambda 5007$ ratio measured by the scanner is at odds with that indicated on the plates. For the other filaments in IC 443 the tie in is poor. It should also be indicated that the runs on which the measures in the red for S 22, S 147, and IC 443 were made was the run in which the dark current of the red cell was extremely high. For the points in NGC 6888 and the Cygnus Loop the tie in appears to be adequate as far as number of readings is concerned, although there is some scatter as illustrated. The only observation that we have reason to question is that for 6960-6. We question it because the correlation between the indicated intensity on the Schmidt plates (as described below) and its adopted H_α magnitude, $8^m.48$, falls off the correlation indicated by 6960-7, 8, 88, and 12, and also because two of the final ratios, H_α/H_β and [OII]/[NII] are out of line compared to the other filaments.

In the reductions of the nebular plates at the microphotometer relatively short, narrow slits were used. As has been noted earlier the emission lines on the nebular plates were not uniform perpendicular to the dispersion and therefore short slits were needed so that the density along the section of the filament being traced at any one time should be reasonably uniform. Although when the density seen by the microphotometer, at any one time, is not uniform, the resulting measure gives the average density for the portion of the filament traced, this

average density is completely unrelated to the average intensity unless the extreme values of density in that portion are both on the linear portion of the H and D curve. Short slits were also deemed necessary, especially in the green, because some of the lines sometimes underwent very striking changes in their relative intensities over short distances on the plates. The actual length of these short slits varied considerably from filament to filament, although they were usually kept fairly uniform for a particular filament. An average length could be taken to be between 20 and 30 seconds of arc. For the nebular plates a slit width, corresponding to approximately 12 microns at the plate was used to be sure that when the slit was centered on the image of the line it also saw a fairly uniform density as far as the width of the line was concerned, and therefore that the actual peak density recorded for a line was not diluted. Although this procedure tended to increase the fluctuations due to the graininess of the emulsion, particularly at clear, it was felt that the resulting accuracy gained by the measures of the peaks of the lines justified the procedure especially since there was always a good deal of clear traced, through which a reasonably good average could be drawn even with the relatively larger fluctuations. In the reductions a single characteristic curve was used for each spectral region. Comparison of the characteristic curves and actual trial reductions using curves from the various wavelengths revealed the error introduced by this procedure to be quite small.

For the stellar plates the relative intensity of the continuum was determined as the wavelength of each nebular line which was being studied.

Using absolute energy distribution curves obtained elsewhere (see above) for the two standard stars, we now obtained the corrections appropriate to the particular plate-filter combination by comparing the true run of the intensity with wavelength with that indicated by the stellar spectrograms. No correction was made in this reduction or in that of the nebular plates for the effect of differential atmospheric extinction; for the lines on any one plate this effect is quite small, except perhaps for the green plates. Since allowance for the atmospheric extinction is made in obtaining the absolute energy distributions, the emulsion sensitivity corrections as obtained above also include a first order correction for the atmospheric extinction. For a sample of the emulsion corrections by which the measured intensities are multiplied see Table 12 of the Appendix.

Since the reduction process for the nebular plates was carried out separately for each of the short lengths of the filaments as discussed above and since for a given filament the integrations connecting the different spectral regions apply only to one of these short lengths, therefore to connect the intensities of, for instance, H_α and $\lambda 5007$ for a section that has not been observed with the scanner, we must take the raw intensity of H_α for the unintegrated length and compare it to the raw intensity of H_α on the same plate for the integrated length; then following the same procedure for $\lambda 5007$ we obtain the relative intensity of H_α, and $\lambda 5007$ for this length which was not observed with the scanner. The one main objection that might be raised against this method is that if placement of the spectrograph slit is not <u>exactly</u> the same for the two

plates and therefore indeed for all plates the variation of intensity along or across the filament can lead to erroneous ratios. To use a gross example, if for the red plate the section of the slit designated as a particular length is on a region that is generally faint in all lines, while for the green plate that same section of the slit is on a bright knot, then we will obtain an erroneously high value of the ratio $\lambda 5007/H_\alpha$. Because of the great deal of very fine structure that is present in the objects being studied here, this situation or certainly a less severe modification of it is not terribly far fetched. In fact examination of the results obtained seems to indicate that it may have happened badly enough to be obvious several times. Thus on NGC 6960-8'(4), of the two ultraviolet plates, one indicates that the intensity of $\lambda 3726$ is 28% of the intensity of $\lambda 3726$ for -8'(2) while the other indicates a ratio of 55%. It is not possible per se to pick either value as correct and so in Table 3 two resulting possible solutions are indicated.

Taking the relative intensities of H_α, $\lambda 5007$, and $\lambda 3726$ derived from the integrations, or the procedure just discussed, we were able to obtain the intensities of all the lines relative to H_α. For the reasons discussed above these relative intensities derived for lines in the green and ultraviolet for sections of the filaments that were not observed with the scanner obviously merit lower weight than those for sections which were observed with the scanner. At this time we also obtained ratios between various other lines that might be of interest, e.g. between [OII] and [OIII] lines. These results for each portion of each filament are listed in Table 3. The values for the line intensities are as observed,

TABLE 3

LINE INTENSITIES

Object	S 22	S 147	S 147	S 147	IC 443	IC 443	IC 443	IC 443	IC 443
Filament	-1'	-1'	-1'	-1'	-6'	-6'	-6'	-6'	-6"
Section	(1)	(2)	(3)	(4)	(1)	(2)	(3)	(4)	(0)
	*		*	*				*	
6731	0.69	0.52	0.53	0.48	0.55	0.62	0.66	0.67	
6716	1.07	0.71	0.75	0.74	0.68)	0.68	0.73	0.92	
6716/6731	1.54	1.36	1.40	1.53	1.22)	1.10	1.12	1.36	
6583	3.08	0.58	0.62	0.57	0.67	0.72	0.53	0.47	
6563	1.00	1.00	1.00	1.00	1.00	1.00	1.00	1.00	
6548	1.51	0.20)	0.21)	0.21)	0.23	0.26	0.19	0.18	
6548/6583	0.49	0.35)	0.35)	0.35)	0.33	0.36	0.35	0.36	
5007		1.02	1.00	1.02	1.10	0.57	0.29	0.21	1.00
4959		0.35)	<	<	0.35	0.19	0.09	<	0.32
4959/5007		0.35)	)	)	0.32	0.34	0.30	)	0.32
4861		0.60	0.58)	0.58)	0.28	0.19	0.18	0.27-0.10	0.32
3869		<0.20	<0.12	<0.14	)	<0.03	<0.03	<0.03	0.08
3729		1.10	1.10	1.13	0.22	0.18	0.10	0.12	0.14
3726		0.85	0.85	0.82	0.19	0.15	0.09	0.10	0.12
3729/3726		1.29	1.28	1.39	1.16	1.16	1.18	1.15	1.14
[OII]/[NII]†					1.3	1.3	1.3	1.3	
[OII]/[OIII]		1.42	1.42	1.42	0.47	0.84	1.10	1.54	0.20
[OII]/[SII]					0.78)	0.95	0.70	0.52	
[SII]/[NII]	0.38	1.58	1.55	1.56	1.38	1.33	1.9	2.44	
H_α/[SII]	0.58	0.81	0.77	0.82	0.81	0.77	0.72	0.63	
H_α/[NII]	0.22	1.28	1.20	1.28	1.11	1.02	1.39	1.54	
H_β/[OIII]		0.45	0.55)	0.55)	0.21	0.27	0.52	0.96-0.36	0.32
H_α/H_β					2.4	2.7	2.5	1.9-5.1	

TABLE 3 (Continued)

Object	IC 443	IC 443	IC 443	IC 443	IC 443	IC 443	IC 443	IC 443	IC 443
Filament	-6"	-6"	-6"	-7'	-7'	-7'	-7'	-7'	-7'
Section	(1)	(2)	(3)	(0)	(1)	(2)	(3)	(4)	(5)
	*						*		
6731	0.68	0.58	0.62	0.57	0.65	0.74	0.75	0.91	0.58
6716	0.70	0.63	0.73	1.00	0.97	1.05	1.05	1.06	0.83
6716/6731	1.02	1.09	1.19	1.75	1.50	1.42	1.43	1.16	1.43
6583	0.63	0.55	0.62	0.54	0.54	0.50	0.51	0.50	0.50
6563	1.00	1.00	1.00	1.00	1.00	1.00	1.00	1.00	1.00
6548	0.16	0.18	0.20	0.18)	0.16	0.16	0.18	0.23	0.16)
6548/6583	0.26	0.33	0.32	0.33)	0.30	0.32	0.33	0.46	0.32
5007	0.33	0.33	0.33 <0.12		<0.06	0.13)	<0.12	<0.08	<0.13
4959	0.13	0.12	0.12 <0.04		<0.02	0.04)	<	<	<
4959/5007	0.40	0.35	0.35		)	)	)	)	)
4861	0.21-0.08	0.22	0.18		0.22	0.24	0.23	0.20	0.27
3869	<0.02	<0.03	)		0.03	<0.03	<0.03		
3729	0.15	0.10	0.11		0.13	0.17	0.17		
3726	0.12	0.07	0.09		0.12	0.13	0.13		
3729/3726	1.25	1.30	1.14		1.12	1.32	1.24		
[OII]/[NII]†	1.3	1.3	1.3		1.3	1.3	1.3		
[OII]/[OIII]	1.14	0.91	1.01		>5.7	2.04	>3.2		
[OII]/[SII]	0.75	0.80	0.80		0.54	0.49	0.51		
[SII]/[NII]	1.75	1.66	1.65	2.12	2.3	2.7	2.6	2.7	2.1
H_α/[SII]	0.72	0.83	0.73	0.64	0.61	0.56	0.56	0.51	0.71
H_α/[NII]	1.27	1.37	1.22	1.35	1.42	1.51	1.45	1.37	1.51
H_β/[OIII]	0.50-0.19	0.54	0.44 >1.2		>3.0	1.6	>1.5	>2.0	>1.6
H_α/H_β	2.5-6.4	1.9	2.4		2.4	2.5	2.5		

TABLE 3 (Continued)

Object	IC 443	IC 443	IC 443	IC 443	IC 443	IC 443	NGC 6888	NGC 6888	NGC 6888
Filament	-15'	-15'	-15'	-16'	-16'	-6'	-1'	-1'	-1'
Section	(1) *	(2)	(3)	(1) *	(2)	(0)	(1)	(2)	(3)
6731	0.53	)	0.49)	0.75	0.71	0.64	<	<	<
6716	0.78	0.87	0.84	0.86	0.87	0.90	<	<	<
6716/6731	1.48	)	1.69	1.15	1.23	1.41	)	)	)
6583	0.65	0.67	0.60	0.71	0.71	0.71	1.44	1.52	1.45
6563	1.00	1.00	1.00	1.00	1.00	1.00	1.00	1.00	1.00
6548	0.20	0.27)	0.28)	0.29	0.29	)	0.57	0.53	0.43
6548/6583	0.31	0.40)	0.47)	0.40	0.41	)	0.40	0.35	0.34
5007	0.20	0.20		0.08)			0.14	0.14	0.12
4959	<	<		0.04			0.05	0.05)	0.04
4959/5007	)	)		0.5)			0.33	)	0.33
4861	0.16-0.08	0.07		0.10			0.09	0.10	0.11-0.08
3869	<0.03	<0.05	<0.05	<0.02			)		
3729	0.10	0.16	0.13	0.07			)		
3726	0.08	0.16	0.10	0.06			)		
3729/3726	1.29	1.03	1.32	1.24			)		
[OII]/[NII]†	1.3	1.3	1.3	1.3					
[OII]/[OIII]	1.67	2.3		3.8					
[OII]/[SII]	0.87		0.83	1.00					
[SII]/[NII]	1.54		1.56	1.61	1.58	1.54)			
H_α/[SII]	0.76		0.79	0.62	0.63	0.65			
H_α/[NII]	1.18	1.06	1.23	1.00	1.00	1.00)	0.50	0.49	0.53
H_β/[OIII]	0.70-0.35	0.28		0.91			0.51	0.58	0.69-0.50
H_α/H_β	2.4-4.8	7.2		3.2			6.0	5.4	5.7)

TABLE 3 (Continued)

Object	NGC 6888	NGC 6888	NGC 6888	NGC 6888	NGC 6888	NGC 6888	NGC 6888	NGC 6888	NGC 6888
Filament	-1'	-1'	-1'	-1'	-2'	-2'	-2'	-2'	-2'
Section	(4)	(5)	(6) *	(7)	(1)	(2) *	(3)	(4)	(5)
6731	<	<	<	<	<	<	<	<	<
6716	<	<	<	<	<	<	<	<	<
6716/6731	)	)	)	)	)	)	)	)	)
6583	1.50	1.48	1.38	1.36	0.42	0.43	0.52	0.40	0.59
6563	1.00	1.00	1.00	1.00	1.00	1.00	1.00	1.00	1.00
6548	0.49	0.65	0.60	0.59	0.15)	0.15	0.18)	0.13)	0.18
6548/6583	0.33	0.44	0.44	0.43	)	0.36	0.35)	)	0.31
5007	0.12-0.06	0.09-0.06	0.09	0.09		0.30	0.29	0.25	0.28
4959	0.04-0.02	0.03-0.02	0.03	0.03		0.12	0.10	0.09	0.10
4959/5007	))	))	0.30	0.33		0.39	0.35	0.36	0.35
4861	0.10	0.09)	0.105	0.10		0.105	0.11	0.09	0.095
3869		<	<	<		<			
3729		0.03	0.03	0.03		0.01			
3726		0.02	0.02	0.03		0.01			
3729/3726		1.20	1.25)	1.04		1.08			
[OII]/[NII]†		0.06	0.08	0.09		0.09			
[OII]/[OIII]		0.7-1.1	0.77	0.92		0.09			
[OII]/[SII]									
[SII]/[NII]									
H_α/[SII]									
H_α/[NII]	0.50	0.47	0.50	0.51	1.8)	1.72	1.43	1.88	1.30
H_β/[OIII]	0.69-0.13	0.82-1.2	0.96	0.90		0.27	0.38	0.28	0.27
H_α/H_β	5.4	6.0)	5.4	5.4		5.4	4.9	6.0	5.7

TABLE 3 (Continued)

Object	NGC 6888	NGC 6960	NGC 6960	NGC 6960	NGC 6960	NGC 6960	NGC 6960	NGC 6960	NGC 6960
Filament	-2'	-2'	-2'	-2'	-3'	-3'	-4'	-4'	-4'
Section	(6)	(1)	(2) *	(3)	(1)	(2) *	(1)	(2) *	(3)
6731	<	<	0.30)	<	<	0.33	0.41	0.33)	0.58
6716	<	<	0.41)	<	<	0.46	0.58	0.51	0.63
6716/6731	)	)	1.36)	)	)	1.38	1.40	1.51)	1.07
6583	0.54	0.50	0.55	0.46	1.05	0.98	0.80	0.82	0.87
6563	1.00	1.00	1.00	1.00	1.00	1.00	1.00	1.00	1.00
6548	0.24	0.17)	0.22)	0.16)	0.41	0.36	0.28)	0.25	0.36
6548/6583	0.44	)	)	)	0.39	0.37	0.35)	)	0.40
5007	0.25	0.49	0.52		0.48	0.44	0.95	1.16	0.98
4959	0.09	0.18	0.21		0.17	0.14	0.29	0.40	0.35
4959/5007	0.34	0.36	0.40		0.35	0.33	0.31	0.34	0.35
4861	0.09	0.20	0.15		0.17	0.16	0.17	0.13	0.15
3869		<0.06	<0.03	<0.05	<0.10	0.14	<0.06	0.13	<0.07
3729		0.46	0.43	0.20	0.54	0.55	0.49	0.54	0.50
3726		0.31	0.31	0.14	0.42	0.41	0.38	0.44	0.45
3729/3726		1.45	1.36	1.40	1.29	1.33	1.28	1.24	1.12
[OII]/[NII]†		1.67	1.39	0.80	0.96	1.03	1.17	1.33	1.12
[OII]/[OIII]		1.41	1.24		1.81	2.02	0.86	0.77	0.87
[OII]/[SII]		1.33	1.52			1.77	1.28	1.71	1.14
[SII]/[NII]			0.92			0.59	0.92	0.78	0.98
H_α/[SII]			1.41			1.27	1.01	1.19	0.83
H_α/[NII]	1.28	1.50	1.28	1.61	0.69	0.75	0.93	0.92	0.81
H_β/[OIII]	0.28	0.31	0.22		0.27	0.29	0.15	0.08	0.11
H_α/H_β	6.0	4.1	5.5		4.8	5.1	4.8	6.3	5.5

TABLE 3 (Continued)

Object	NGC 6960	NGC 6960	NGC 6960	NGC 6960	NGC 6960	NGC 6960	NGC 6960	NGC 6960	NGC 6960
Filament	-4'	-6'	-6'	-6'	-7'	-7'	-7'	-7'	-8'
Section	(4)	(0)	(1)	(3)	(1)	(2)	(3)	(4)	(1)
			*			*			*
6731	<0.47		0.45	<0.29	0.65	0.56)	0.40)		0.68
6716	0.51		0.52	0.50	0.80	0.70)	0.43)		0.95
6716/6731	>1.08		1.15	)	1.30)	1.24)	1.06)		1.40
6583	0.75		0.99	0.79	0.78	1.03	0.95		0.89
6563	1.00		1.00	1.00	1.00	1.00	1.00		1.00
6548	0.25)		0.33	0.30)	0.26	0.38	0.33		0.28
6548/6583	)		0.33	)	0.33	0.37	0.35		0.31
5007	1.18	1.00	0.24	<0.03	0.31	0.33	0.76	1.00	0.59
4959	0.43	0.36	0.08	<0.01	0.09	0.12	0.27	0.33	0.20
4959/5007	0.37	0.36	0.34	)	0.28	0.37	0.36	0.33	0.34
4861	0.18	0.26	0.08	0.09	0.15	0.15	0.14	0.06	0.14
3869	<0.08	<0.02	<0.03	<0.03	0.07	0.05	0.12	0.12	
3729	0.57	0.88	0.29	0.13	0.39	0.53	1.06	0.70	
3726	0.45	0.67	0.24	0.11	0.27	0.42	0.87	0.56	
3729/3726	1.26	1.30)	1.23	1.14	1.41	1.27	1.21	1.23	
[OII]/[NII]†	1.48		0.58	0.32	0.91	0.97	2.19		
[OII]/[OIII]	0.77	1.40	2.02	>7	2.02	2.58	2.29	1.16	
[OII]/[SII]	>1.46		0.80	>0.44	0.66	1.09)	3.38)		
[SII]/[NII]	<0.98		0.74	<0.74	1.40	0.89)	0.65)		1.40
H_α/[SII]	>1.02		1.03	1.26	>0.69	0.79)	1.20)		0.61
H_α/[NII]	1.00		0.76	0.92	0.96	0.71	0.78		0.85
H_β/[OII)	0.11	0.20	0.25	>2.3	0.40	0.34	0.15	0.05	0.19
H_α/H_β	4.6		9.8	9.0	5.5	5.5	5.8		5.8

TABLE 3 (Continued)

Object	NGC 6960	NGC 6960	NGC 6960	NGC 6960	NGC 6960	NGC 6960	NGC 6960
Filament	-8'	-8'	-8'	-12'	-12'	-12'	-12'
Section	(2)	(3)	(4)	(1)	(2)	(3)	(4)
	*					*	
6731	0.27	<0.41	0.79	0.48		0.47	0.53
6716	0.37	0.67	0.80	0.60		0.59	0.60
6716/6731	1.36	>1.63	1.01	1.27		1.25	1.14
6583	0.82	0.64	0.89	0.74		0.72	0.75
6563	1.00	1.00	1.00	1.00		1.00	1.00
6548	0.19	0.33	0.24)	0.22		0.22	0.25
6548/6583	0.23	0.52	0.27)	0.30		0.30	0.34
5007	5.07	4.00	6.40	0.36	1.00	0.29	0.31-0.78
4959	2.18	1.33	1.92	0.13	0.36	0.11)	0.10-0.25
4959/5007	0.43	0.33	0.30	0.35	0.36	0.38)	0.32
4861	0.38)	0.34)	0.32)	0.17	0.94	0.17-0.11	0.15
3869	0.37	0.25	<	<0.04	<	0.05	0.08
3729	0.99	0.88	0.50-1.01	0.34	2.25	0.36	0.38
3726	0.79	0.53	0.38-0.74	0.27	1.82	0.30	0.31
3729/3726	1.25	1.67	1.36	1.28	1.23	1.20	1.22
[OII]/[NII]†	2.55	2.10	1.13-2.26	0.93		1.01	1.00
[OII]/[OIII]	0.31	0.32	0.13-0.27	1.52	3.7	2.02	2.06-0.82
[OII]/[SII]	4.05	>1.9)	0.80)-1.60)	0.82		0.91	0.89
[SII]/[NII]	0.63	1.11)	1.41)	1.12		1.13	1.13
H_α/[SII]	1.56	0.93)	0.63)	0.93		0.94	0.88
H_α/[NII]	0.99	1.03	0.89	1.04		1.06	1.00
H_β/[OII]	0.05	0.06	0.04	0.36	0.72	0.44-0.28	0.37-0.16
H_α/H_β	2.1)	2.4)	2.4)	4.8		4.8-7.4	5.2

TABLE 3 (Concluded)

† Reddening corrections have been applied to these ratios.

Remarks:

1) no reddening correction has been applied to S 22 and S 147.

2) < sign indicates upper limit.

3)) sign indicates poor quality.

4) * indicates this section has been observed with the scanner.

5) Line between 5007 and 6548/6583 indicates poor tie-in between spectral regions.

uncorrected for reddening, while the ratios between doublets as listed in the lower part of the table are corrected for reddening.

Apart from the difficulties with the calibration between spectral regions and uncertainty in the reddening correction, the scatter of the results from two plates of the same filament indicates that the uncertainty of a given value in the table varies between 10% or less for lines that appear strong on the plates (before emulsion corrections are applied) e.g. λ6583 and frequently H_β, and 30% for lines which appear weak on the plates, e.g. the [SII] doublet and sometimes H_β.

In order to check the uncertainty due to inaccuracies in the reading of the microphotometer tracings, the intensities from one plate were altered by amounts corresponding to the estimated reading errors and then reduced. The results for all cases, including shifts of clear, continuum and line peak intensities were unchanged. For changes in the emulsion correction corresponding to the size of the maximum scatter of the observed points around the mean correction, perceptible changes were observed but again were small compared to some of the plate to plate scatter.

All measures of the plates for radial velocities were made on the same measuring engine used by Wilson et al. (1959) in their study of the motions of the Orion Nebula. On this measuring engine there is provision for motion perpendicular to the dispersion so that measures can be made on the top comparison, any point on the nebular emission lines and the bottom comparison separately. In order to minimize the effect of temperature changes on the measuring engine all measures were made in a sub-basement room and the lights were kept burning continuously.

In keeping with fairly common practice an uncertainty of plus or minus one micron was assumed in the measured position of each line. Although general agreement among measures seems to be of this order, this assumption may be a bit optimistic since the nebular lines were frequently rather irregular and the widths of the heavier emission lines, which still had to be used, were frequently 20 microns. With a dispersion of 240 A/mm an uncertainty of one micron is equivalent to an uncertainty of 0.24 A which at λ6600 is equivalent to an uncertainty of 11 km/sec. The wavelengths used for the forbidden lines were those given by Bowen (1955).

The first problem to surmount in measuring the nebular plates to obtain radial velocities was the question of the apparent curvature of the slit on the plates. Minkowski (1942) has treated the question of slit curvature in grating spectrographs and on the basis of his work a correction of 4 microns would be predicted for the middle of the slit on our red plates and a similar correction of 8 microns for our ultraviolet plates. The correction is in the sense that the slit appears to bow toward the violet end and so the correction must be added to the readings of the nebular lines so as to shift them to the red. To check this figure for the curvature, exposures for each spectral region were made, in which the comparison spectrum was passed through both the comparison windows and the nebular window. These plates were then measured to determine the curvature. For the red plates the maximum correction indicated by the measures was 4 microns--very much in accord with the predictions of theory. Using a correction curve as predicted by Minkowski and

checked by the test exposure, two red plates were measured for each filament. For various reasons the green and ultraviolet plates were not considered satisfactory for radial velocity measures. In general no attempt was made to measure the separate sections of the filament but one section was chosen and measured. In one or two cases, however, measures were made of each section and these showed a scatter rather comparable with that found from filament to filament. Of the nebular lines only four at most were available, since λ6731 is located beyond the end of the Neon comparison. Of the four, frequently only two were bright enough to measure, especially in the Cygnus Loop where the λ6717 is weak; λ6548 is usually rather weak unless H_α is very heavily exposed. With the comparison lines we fared little better. For plates on which just the [NII] lines and H_α were measured we had only four comparison lines and even when the measures were extended to include λ6717 we still only had six comparison lines. This leaves only two or four measures to determine the dispersion curve. Because this left the dispersion curve so poorly determined, especially for those plates on which λ6717 could not be measured, it was drawn in with a french curve as a fairly set shape whose amplitude was adjusted to fit the two points. The amplitude of the resulting curves ranges between approximately 0.2 and 0.4 A for the plates on which only four comparison lines were measured. For three plates the dispersion curve was completely indeterminate; their radial velocities are listed as question marks. Sun Reductions were obtained from the Mt. Wilson program.

On some plates there were large differences of 40 or more km/sec in the velocity indicated by two lines. When three or more lines were

available in this situation, the average of the lines was taken giving half weight to the dissident value. Fortunately this situation never arose when only two lines were measured. The final values of the Heliocentric radial velocities for the individual plates of each filament are listed in Table 4. It should be remembered that the uncertainty of these values is around 10 km/sec.

Reduction of the new second epoch plate of IC 443 was done through comparison with the first epoch plate obtained by Baade in 1939 by using the Kapteyn blink comparator at the Mt. Wilson offices. This instrument has a movable reticle at the eyepiece so that the two plates can be aligned using the stars and then measured separately to determine the difference in the location of a filament. Measurements of the motion of the edges of the filaments were badly prejudiced due to the fact that the filaments were slightly wider on the second plate than on the first epoch plate due both to the fact that the seeing was not as good when the second plate was taken and also to the fact that the exposure on the second plate was a bit heavier. Measures were therefore made on the centers of the filaments--a slightly uncertain procedure since the filaments are not completely sharp. A mean motion of several of the filaments in the N. E. quadrant (where the first epoch plate was taken) was determined finally as

$$0.''015 \text{ per year}$$

with an estimated error of probably $\pm$ 50%. For comparison the proper motion of expansion of IC 443 was estimated by Minkowski (1958) as being of the order of $0.''01$ per year. The plates used for this measurement

TABLE 4

HELIOCENTRIC RADIAL VELOCITIES (km/sec)

Object	V_R	V_R
S 22-1	-22	
S 147-1	+47	+38
IC 443-6'	-15	-10
IC 443-6"	+ 4	+19
IC 443-7'	-24	-20
IC 443-15'	+30	+33
IC 443-16'	+28	
NGC 6888-1'	-38	-53
NGC 6888-2'	-20	-30?
NGC 6960-2'	+ 6	?
NGC 6960-3'	- 8	+20
NGC 6960-4'	?	?
NGC 6960-6'	+ 6	+32
NGC 6960-7'	- 2	+ 8
NGC 6960-8'	+ 1	
NGC 6960-12'	-14	- 1

were taken 14 years apart. Some evidence was also found from the measures of the edges of the filaments for belief that some of the filaments have shown virtually no motion in 22 years.

In the reductions of the Schmidt plates of these objects to obtain values for the net monochromatic flux direct intensity tracings were obtained. In tracing the plates the microphotometer slit was set to be equivalent to the size of the scanner slit used in the integration work. Scans were made in contiguous strips (200 for the section of the Cygnus Loop comprising NGC 6992 and 6995). The weaker, short exposure plates were used in this work since all points then fell on the linear portion of the characteristic curve and thus the fact that the microphotometer slit was virtually always unevenly illuminated did not matter. The resulting records were then integrated with a planimeter to find the area under the tracings. Peaks due to stars were eliminated as much as possible; this task was not too difficult since in most cases there is a difference in the shape of the peaks due to filaments and the shape of the peaks due to star images. The total area for the integrations was then divided by the effective slit width to yield a total equivalent deflection. To calibrate the intensity scale, the deflection or indicated intensity was determined at each of the positions which had been measured with the scanner. To determine the flux at the plate in H_a alone, we need to know the sensitivity of the plate filter combination and the relative intensities of the [NII] lines and H_a. To determine the sensitivity of the 103_aE plus OR-1 combination, exposures were made in the standard star program with 103_aE plates cut from a Schmidt

plate. Since no OR-1 filter is available for the spectrograph these exposures were made with the OG filter and when its effect was later removed the result was the sensitivity of the 103_aE emulsion influenced perhaps by the spectrograph in an undetermined manner. The transmission of the OG filter is actually flat through the region of interest. The transmission of the OR-1 filter was taken from the filter catalogue. The resulting function is

$$I(103_aE + OR\text{-}1) = 0.845\, I(6584) + I(H_\alpha) + 1.08\, I(6548),$$

which can be converted to a function of $I(H_\alpha)$ for any one filament section since we also know the intensity of λ6583 and 6548 relative to H_α.

Having now determined $I(103_aE + OR\text{-}1)$ as a function of $I(H_\alpha)$ for a given location we can correct the measured intensity from that location to the intensity due to H_α alone, e.g. if $I(103_aE + OR\text{-}1) = 2.0\, I(H_\alpha)$ then we will divide the intensity measured from the plate by 2 to get the intensity due to H_α. This new value can now be compared to the absolute intensity of H_α at that location as determined by the scanner, and the correlation between the two intensity scales obtained. Before we find the flux in H_α from the whole object being considered we must repeat the routine by finding the average value of $I(103_aE + OR\text{-}1)/I(H_\alpha)$ for all filaments observed in the object and then correcting the total deflection which had been previously determined. The objects for which this was carried out were S 22, IC 443, NGC 6888, and NGC 6992 and 6995 in the Cygnus Loop. The results for the four objects measured are listed in Table 5.

TABLE 5

MONOCHROMATIC FLUXES

Object	NGC 6992 & 6995	NGC 6888	S 22	IC 443
Total observed flux in H_α (ergs/cm^2/sec)	4.4×10^{-9}	1.55×10^{-9}	6.4×10^{-11}	3.2×10^{-9}
Total observed flux in H_α corrected for space absorption (ergs/cm^2/sec)	6.2×10^{-9}	4.5×10^{-9}		13×10^{-9}
Observed radio flux at 1000 megacycles (ergs/cm^2/sec/(c/s))	26×10^{-23}			195×10^{-23}
Distance (parsecs)	770	1600		a) 2000 b) 800
Total loss in H_α (ergs/sec)	4.2×10^{35}	13×10^{35}		a) 50×10^{35} b) 8×10^{35}

CALCULATIONS

In order to interpret the various line intensity ratios and connect them with the physical conditions of temperature, density, excitation and abundances, calculations must be made which, for given values of the physical parameters, predict the line ratios that would be observed. Such calculations for the case of collisional excitation and ionization were carried out for the lines studied.

The intensity of an emission line between levels n and m, I_{nm}, can be written as

$$I_{nm} = N_n A_{nm} h\nu_{nm} .$$

The atomic constants are supposedly known and the main astrophysical problem is the calculation of the population, N_n, in the excited state. All the forbidden lines studied in this program are lines arising from the lowest excited level and are optically thin. Since induced emissions, and reabsorptions are negligible the only means of populating the excited level from which the forbidden lines arise are collisional excitations from a lower state or collisional or radiative deexcitations from a higher state. The rate of collisional excitation or deexcitation, q_{nm}, is given by

$$q_{nm} = N_e v_e Q_{nm}$$

where Q_{nm} is the collisional cross-section, and v_e is the velocity of the incident electron. The cross-sections, Q_{nm} may be conveniently expressed in terms of the dimensionless, symmetrical

parameter Ω_{nm}, introduced by Hebb and Menzel (1940) and called the collision strength (Seaton 1953) as

$$\Omega_{nm} = \left(\frac{2\pi m_e v_e}{h}\right)^2 \cdot \frac{\omega_n}{\pi} \cdot Q_{nm}$$

where ω_n is the statistical weight of state n. Values of the quantities Ω_{nm} and ω_n are listed in Table 13 of the Appendix as given by Seaton (1954 and 1958).

Assuming a Maxwellian velocity distribution, and that the collision strengths are independent of electron energy, we then have (Seaton 1960), collecting constants for the case $E_n > E_m$

$$q_{nm} = 8.63 \times 10^{-6} \frac{N_e \Omega_{nm}}{\omega_n T_e^{1/2}}$$

For the case of collisional excitation with detailed balancing in the collisional processes we can also write down

$$q_{mn} = 8.63 \times 10^{-6} \frac{N_e \Omega_{nm}}{\omega_m T_e^{1/2}} \cdot \exp\left(-E_{nm}/kT_e\right)$$

where the exponential enters because of the fact that not all of the electrons have sufficient energy to excite the transition. This last equation is strictly not descriptive of the case at hand since it implies the lack of radiative deexcitations. We will see however that the effect of these deexcitations from the second excited state is small.

Neglecting induced emissions and radiative excitations from the ground state we can for a three level atom write the equations of detailed balancing between transitions into and out of a given state as

$$N_2(A_{21}+q_{21}+q_{23}) = N_1q_{12}+N_3(A_{32}+q_{32})$$

and

$$N_3(A_{31}+A_{32}+q_{31}+q_{32}) = N_1q_{13}+N_2q_{23}$$

so that eliminating N_3 we obtain

$$\frac{N_2}{N_1} = \frac{q_{12}+q_{13}(A_{32}+q_{32})/(A_{31}+A_{32}+q_{31}+q_{32})}{A_{21}+q_{21}+q_{23}(A_{31}+q_{31})/(A_{31}+A_{32}+q_{31}+q_{32})}$$

where the A's are again the Einstein coefficients for spontaneous emission and are also listed in Table 13 of the Appendix from Seaton. With regard to the fact that in writing down the expression for the rate of collisional excitations we have assumed detailed balancing in the collisional processes, note that since for the temperatures and densities considered in the program q_{12} is always much larger than the rest of the numerator then the influence of radiative deexcitations in populating the first excited state are negligible. If the assumption is made that all the atoms or ions in a particular stage of ionization are in levels 1 and 2, we can go further and express N_2 in terms of the total number of atoms in the particular stage of ionization. This assumption is valid since most of the atoms are in the first level.

In order to go further still and tie the number of atoms in level 2 of the particular stage of ionization to the total number of atoms of that element, we must know the population of the various stages of ionization of the element. The calculation of the degree of ionization in interstellar matter is generally a difficult thing because allowance must be made for the dilution and possible reddening of the radiation of the exciting star

as well as the character of the radiation. For the case in which the ionization is not due to radiation but collisions a relatively simple formula has been developed (Elwert 1952) for the case of detailed balancing where only the processes of photorecombination and collisional ionization through electron collisions are important in the ionization equilibrium. Therefore since the number of photorecombinations, N_{pr}, to state i from state $i+1$ is given by

$$N_{pr} = n_{i+1} N_e Q_{21}$$

where Q_{21} will be a complicated function of atomic constants and the physical conditions. The number of collisional ionizations, N_{ci}, from state i to state $i+1$ is given by

$$N_{ci} = n_i N_e S_{12}$$

where S_{12} like Q_{21} is a complicated function of atomic constants and physical conditions. Equating N_{ci} and N_{pr} we find

$$\frac{N_{i+1}}{N_i} = \frac{S_{12}}{Q_{21}} .$$

Derivations of the form of S_{12} and Q_{21} are presented by Elwert (1952) and lead to an equation

$$\frac{N(X^+)}{N(X)} = C \frac{\zeta_n}{n} \left(\frac{\chi_n}{\chi_H}\right)^{-2} \left(\frac{\chi_n}{kT}\right)^{-1} \exp(-\chi_n/kT)$$

where we have consolidated atomic constants in the constant C. By fitting this equation to calculations of Chamberlain (1953a), Miyamoto

(1956) obtains a value of 6×10^5 for C. We adopt this value for our computations. Here N(X) represents the number of parent atoms, or ions. C is used here as a constant of proportionality and adopted as 6×10^5 following Miyamoto. ζ_n is the number of electrons in the outermost shell, n, of the parent atom or ion. χ_n and χ_H are the ionization potentials of the parent ion and Hydrogen, respectively. T is the ionization temperature and is here identical to the electron temperature. Through suitable use of the above expressions we should be able to calculate the intensity of a given line, or doublet, with respect to the total number of atoms of that element. The ionization potentials used were obtained from Moore (1945 and 1949) and are listed in Table 14 of the Appendix.

In order to calculate the intensity of the Balmer lines we must obtain an expression for N_n for Hydrogen. Such an expression is well known and can be obtained by dividing the Boltzmann equation for Hydrogen by the Saha equation for Hydrogen to yield

$$N_n = N_p N_e \frac{h^3}{(2\pi m k T_e)^{3/2}} n^2 b_n \exp(X_n / kT_e)$$

where b_n is introduced to take account of the departures from thermodynamic equilibrium, and X_n is the difference between the excitation potential of level n and the ionization potential of Hydrogen. b_n is a function of the electron temperature, and also depends on whether the filaments are optically thick to Lyman radiation and other conditions. The values of b_n for three temperatures, 10^4, 2×10^4, and 4×10^4 ^oK, and for various cases have been calculated by Chamberlain (1953) with

emphasis on slow collisions. The values for b_3 and b_4 for the case where the filaments are optically thick to Lyman radiation and the cause of excitation is collisional are copied in Table 15 of the Appendix.

The doublet ratios for [NII], and [OIII], are fixed at 0.34 and 0.35 respectively by their transition probabilities since in this case the two lines both arise from the same fine structure level. On the other hand the lines in the [OII] and the [SII] doublets arise from different levels of the same term (see below).

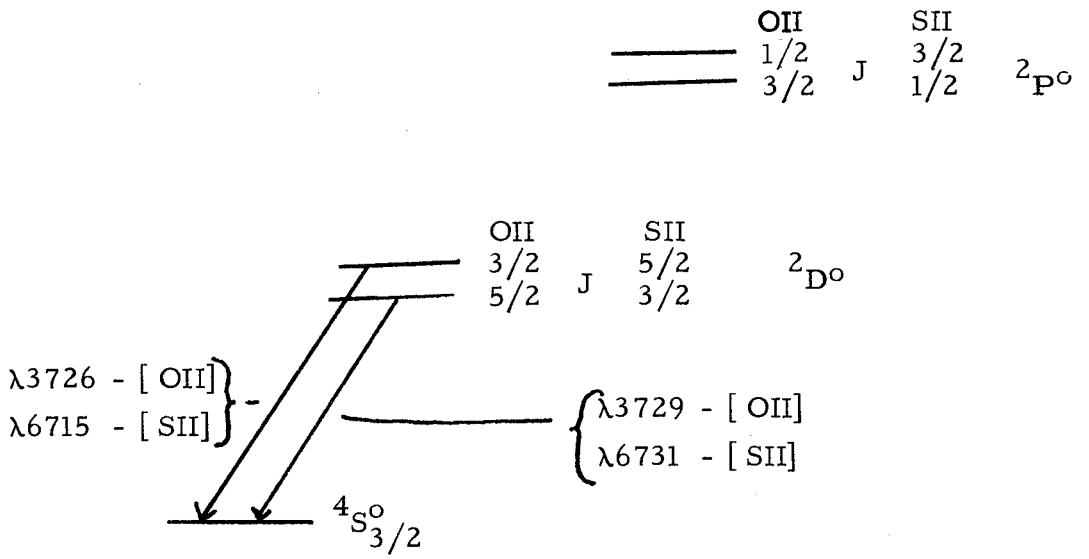

Figure 4: The fine structure of the ground configuration of OII, and SII

Since the two levels of the doublet are of very nearly the same energy, the ratios of their populations are not a sensitive function of the temperature. Since the cross-sections and transition probabilities of the two levels are different the ratio of their populations, and hence the intensities of the lines is a function of the electron density. Thus neglecting

differences in statistical weight between the levels as long as the electron density is high enough so that collisional deexcitations are much more important in depopulating the levels than radiative transitions, $\lambda 3726$ will be more intense than $\lambda 3729$ because of the fact that the transition probability for $\lambda 3726$ is larger than that for $\lambda 3729$. Once the density has become low enough so that collisional deexcitation is not likely to take place before radiative deexcitation can occur then the intensity of the two lines will be governed solely by the number of atoms arriving at the two levels since all of these atoms will return to the ground state by the emission of the forbidden lines. Therefore in this case $\lambda 3729$ will be more intense than $\lambda 3726$ because the cross-section for collisional excitation from the ground state to the $^2D_{5/2}$ level is larger than that for the $^2D_{3/2}$ level.

As derived above for the total intensity of a doublet, we can extend the equation for the intensity of a line as a function of N_n to indicate the ratio from two levels d and d' as

$$r = \frac{I(d' - s)}{I(d - s)} = \frac{N_{d'}}{N_d} \cdot \frac{A(d' - s)}{A(d - s)} \cdot \frac{h\nu(d' - s)}{h\nu(d - s)}$$

and therefore as before the main problem is determining the value of $N_{d'}/N_d$.

Considering a steady state, ignoring transitions between levels of the same doublet term, neglecting deexcitations from the ^2P term and assuming that the collisional strength for the transition from one level of a term to another term is proportional to the statistical weights of the level involved so that

$$\frac{\Omega(A_j, B)}{\omega_j} = \frac{\Omega(A_{j'}, B)}{\omega_{j'}} = \frac{\Omega(A, B)}{\omega_j + \omega_{j'}}$$

where A and B are two terms and A is split into two levels j and j', we can write the equation of equilibrium for detailed balancing for a four level atom as

$$N_S q_{Sd} = N_d(q_{dP} + q_{dS} + A_{dS})$$

and

$$N_S q_{Sd'} = N_{d'}(q_{d'P} + q_{d'S} + A_{d'S}) .$$

Following Naqvi and Telwar (1957) we indicate the two levels $^2D_{3/2}$ and $^2D_{5/2}$ by d and d' respectively. We have also in writing down these expressions made the same assumptions stated earlier about the lack of importance of reabsorption and induced emission. Eliminating N_S we can solve for $N_{d'}/N_d$ as

$$\frac{N_{d'}}{N_d} = 1.5\ \frac{CN_e(\Omega_{SD} + \Omega_{DP} \cdot \exp(-\chi_{DP}/kT_e)) + \omega_D A(d-s)}{CN_e(\Omega_{SD} + \Omega_{DP} \cdot \exp(-\chi_{DP}/kT_e)) + \omega_D A(d'-s)}$$

where C is $8.63 \times 10^{-6}/T_e^{1/2}$ and the other symbols have their usual meanings. Values for the Einstein A's given by Naqvi and Telwar are listed in Table 16 of the Appendix. The values of A for the [SII] lines are due to Garstang (1952). The collision strengths have been previously listed in Table 13 of the Appendix. There $\Omega(1, 2)$ is equivalent to Ω_{SD}.

Using new and presumably improved values of the transition probabilities (adjusted to give the observed high density limit) and

collision strengths, and taking into consideration transitions between levels of the same term and the population of the third term, Osterbrock and Seaton (1957) derived an expression for the ratio of the [OII] doublet, I(3729)/I(3726), as

$$r = 1.5\,\frac{1 + 0.33\epsilon + 2.30x(1 + 0.75\epsilon + 0.14\epsilon^2)}{1 + 0.40\epsilon + 9.9x(1 + 0.84\epsilon + 0.17\epsilon^2)} \quad \text{for } x \ll 290$$

where $\epsilon = \exp(-1.96 \times 10^4/T_e)$ and $x = 10^{-2}\, N_e/T_e$. Calculations for [OII] based on the expression of Osterbrock and Seaton were accepted as superior to those based on the expression of Naqvi and Telwar since the former represent a more complete approach. No expression for the [SII] doublet exists except for Naqvi and Telwar and so their expression had to be used for that doublet. At the same time, as a comparison, calculations were also carried out for the [OII] doublet using the Naqvi and Telwar relation.

Calculations were carried out for 22 values of the density between 1000 and 80 electrons per cm^3 inclusive, for each of 8 values of the temperature between 10^4 and 10^5 ^oK inclusive. The general procedure of the program using the expressions derived above was as follows. First the degree of ionization was obtained for the collisional case for each element for each temperature for the first seven stages. The proportion of the total number of atoms of each element in each stage is listed in Table 6. Note that even at 10^5 ^oK we have thus included in these stages virtually all the atoms of a given element. Next, using the ionization results and the data listed earlier with the equation for N_2/N_1, the rate of emission in ergs per second per atom was calculated for each line or

TABLE 6

IONIZATION $N = A \times 10^{-n}$

	T_e (°K)	XI/X		XII/X		XIII/X		XIV/X		XV/X		XVI/X		XVII/X	
		A	(n	A	(n	A	(n	A	(n	A	(n	A	(n	A	(n
Hydrogen	10^4	0.99		0.57	(2										
	1.5×10^4	0.38		0.62											
	2×10^4	0.33	(1	0.97											
	3×10^4	0.16	(2	1.00											
	4×10^4	0.33	(3	1.00											
	6×10^4	0.60	(4	1.00											
	8×10^4	0.23	(4	1.00											
	10^5	0.13	(4	1.00											
Nitrogen	10^4	0.996		0.39	(2	0.40	(3	0.86	(34						
	1.5×10^4	0.39		0.61		0.85	(6	0.23	(18	0.70	(42				
	2×10^4	0.28	(1	0.97		0.54	(3	0.18	(11	0.23	(28				
	3×10^4	0.93	(3	0.80		0.20		0.94	(5	0.57	(15	0.32	(29		
	4×10^4	0.32	(4	0.15		0.85		0.51	(2	0.74	(9	0.71	(19		
	6×10^4	0.13	(6	0.36	(2	0.53		0.46		0.18	(3	0.33	(9		
	8×10^4	0.13	(8	0.96	(4	0.79	(1	0.90		0.20	(1	0.54	(5		
	10^5	0.40	(10	0.58	(5	0.14	(1	0.78		0.20		0.12	(2		

TABLE 6 (Continued)

	T_e (^oK)	XI/X		XII/X		XIII/X		XIV/X		XV/X		XVI/X		XVII/X	
		A	(n	A	(n	A	(n	A	(n	A	(n	A	(n	A	(n
Oxygen	10^4	0.98		0.17	(1	0.21	(15	0.68	(40						
	1.5×10^4	0.17		0.83		0.12	(7	0.88	(23	0.41	(46				
	2×10^4	0.11	(1	0.99		0.17	(4	0.64	(15	0.13	(31				
	3×10^4	0.54	(3	0.98		0.22	(1	0.49	(7	0.45	(17	0.66	(34		
	4×10^4	0.60	(4	0.54		0.46		0.28	(3	0.61	(10	0.71	(22	0.21	(37
	6×10^4	0.44	(6	0.22	(1	0.83		0.15		0.86	(4	0.91	(11	0.25	(20
	8×10^4	0.64	(8	0.82	(3	0.23		0.75		0.25	(1	0.85	(6	0.25	(12
	10^5	0.15	(9	0.36	(4	0.34	(1	0.70		0.27		0.32	(3	0.63	(8
Sulfur	10^4	0.47		0.53		0.12	(7	0.93	(22	0.13	(42				
	1.5×10^4	0.11	(1	0.99		0.28	(3	0.23	(11	0.41	(24	0.46	(46		
	2×10^4	0.11	(2	0.97		0.33	(1	0.31	(6	0.69	(15	0.13	(30		
	3×10^4	0.18	(4	0.18		0.81		0.10	(1	0.31	(6	0.10	(15	0.23	(28
	4×10^4	0.33	(6	0.11	(1	0.67		0.32		0.13	(2	0.62	(9	0.94	(18
	6×10^4	0.25	(9	0.35	(4	0.29	(1	0.62		0.35		0.29	(3	0.33	(8
	8×10^4	0.71	(12	0.22	(6	0.75	(3	0.11		0.86		0.31	(1	0.33	(4
	10^5	0.84	(14	0.44	(8	0.37	(4	0.19	(1	0.71		0.26		0.45	(2

Remarks: Where n is omitted it is zero.

doublet of interest as a function of the values of N_e and T_e. The calculations for Hydrogen we performed using the b_n's calculated by Chamberlain (1953a) for the collisional case in which the nebula is optically thick to Lyman radiation. In the Hydrogen calculations we were therefore restricted to the three values of the temperature for which the collisional b_n's were available. The intensities for all the lines and doublets were printed out and are available, however only those for H_α are presented here in complete form because of their use in connection with the monochromatic fluxes derived from the Schmidt plates. See Table 17 in the Appendix. In Table 7, as an example, we list the calculated intensities per atom per second of each doublet for each temperature but just for $N_e = 400$ -- for other values of the density the intensities are approximately linear functions of N_e. Following this, ratios were obtained between lines or doublets of interest. The results are presented in Table 8 for the Balmer decrement and in Figures 5 - 10 for the other ratios. The values of these ratios are very insensitive to changes in density and so the results are displayed at an arbitrary density. Once the temperatures are known total abundances of the elements with respect to one another should be able to be determined using these values of the ratios between the lines and doublets since the ratio between the observed and predicted ratios is, for the proper temperature, just the relative abundance.

Finally calculations were made of the values of the two doublet ratios $\lambda 6731/\lambda 6716$ and $\lambda 3729/\lambda 3726$. As indicated above these calculations were carried out using both the formulation of Naqvi and Telwar

TABLE 7

I(X) [ergs/sec/atom] AT $N_e = 400\ cm^{-3}$

$I = A \times 10^{-n}$

$T_e \times 10^{-4}$	[OII]		[OIII]		[NII]		[SII]		H_α		H_β	
	A	(n	A	(n	A	(n	A	(n	A	(n	A	(n
10	0.54	(21	0.21	(18	0.41	(22	0.63	(25				
8	0.12	(19	0.14	(17	0.71	(21	0.33	(23				
6	0.32	(18	0.54	(17	0.28	(19	0.56	(21				
4	0.68	(17	0.29	(17	0.12	(17	0.18	(18	0.15	(21	0.37	(22
3	0.10	(16	0.12	(18	0.59	(17	0.27	(17				
2	0.63	(17	0.69	(22	0.60	(17	0.13	(16	0.55	(21	0.11	(21
1.5	0.31	(17	0.35	(27	0.30	(17	0.10	(16				
1.0	0.20	(19	0.28	(33	0.11	(19	0.32	(17	0.09	(22	0.16	(23

TABLE 8

$I(H_\alpha)/I(H_\beta)$ FOR NEBULA OPTICALLY THICK TO THE LYMAN LINES

T_e	4×10^4	2×10^4	10^4	
	4.07	4.80	5.77	Collisional Excitation
	2.43	2.59	2.50	Radiative Excitation (Case B)

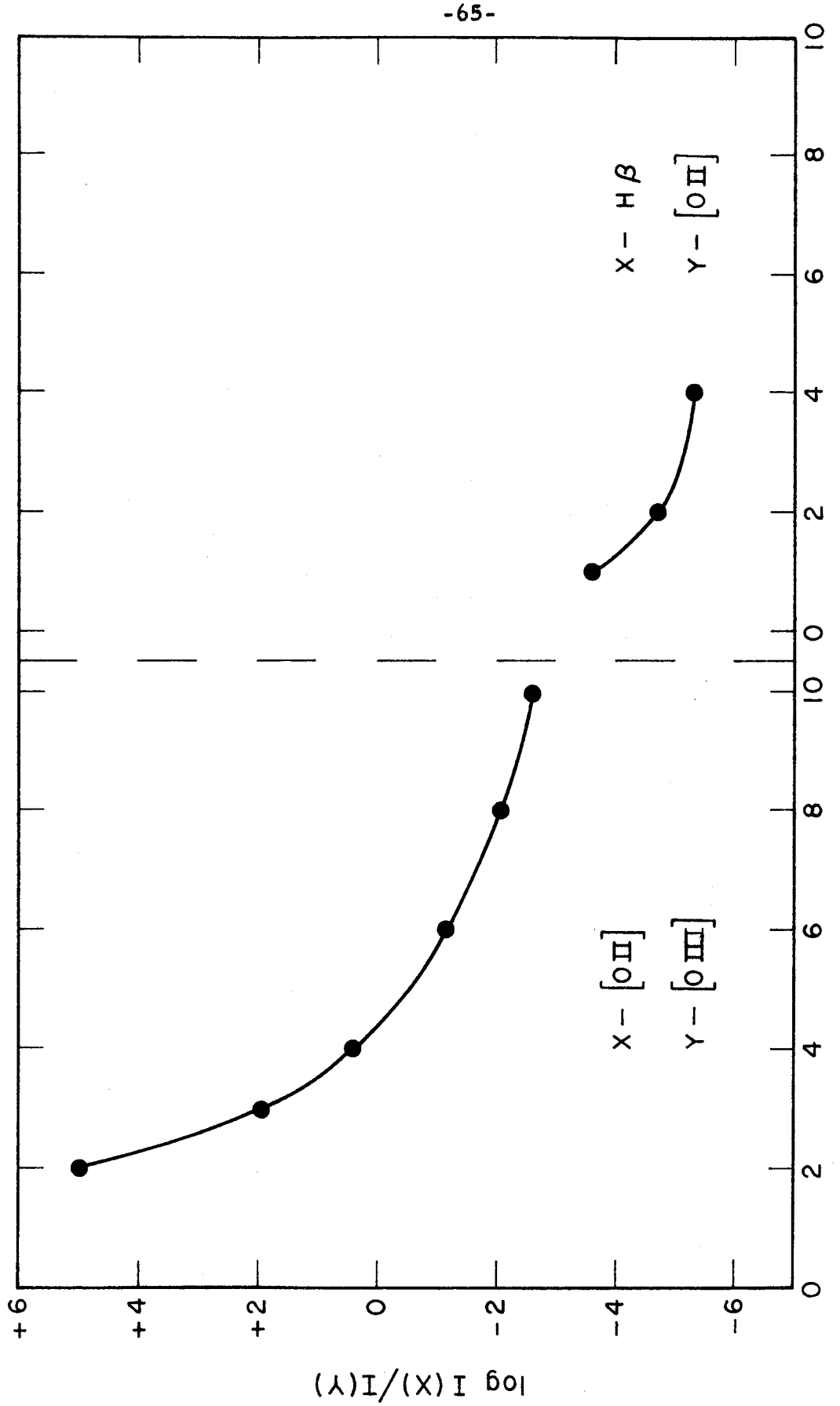

Figure 5
Relative intensities for equal numbers of atoms.

Figure 6

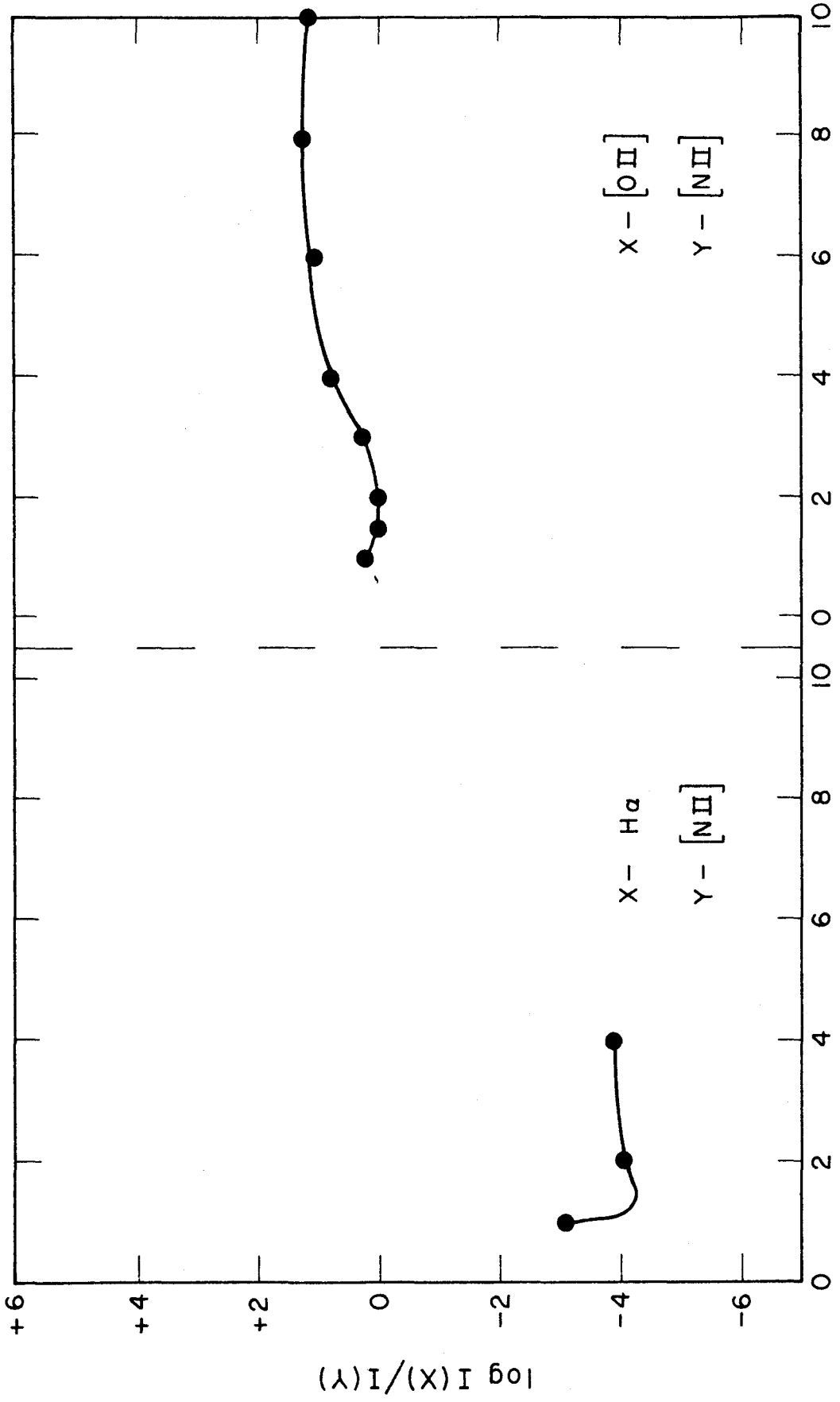

Figure 7
Relative intensities for equal numbers of atoms.

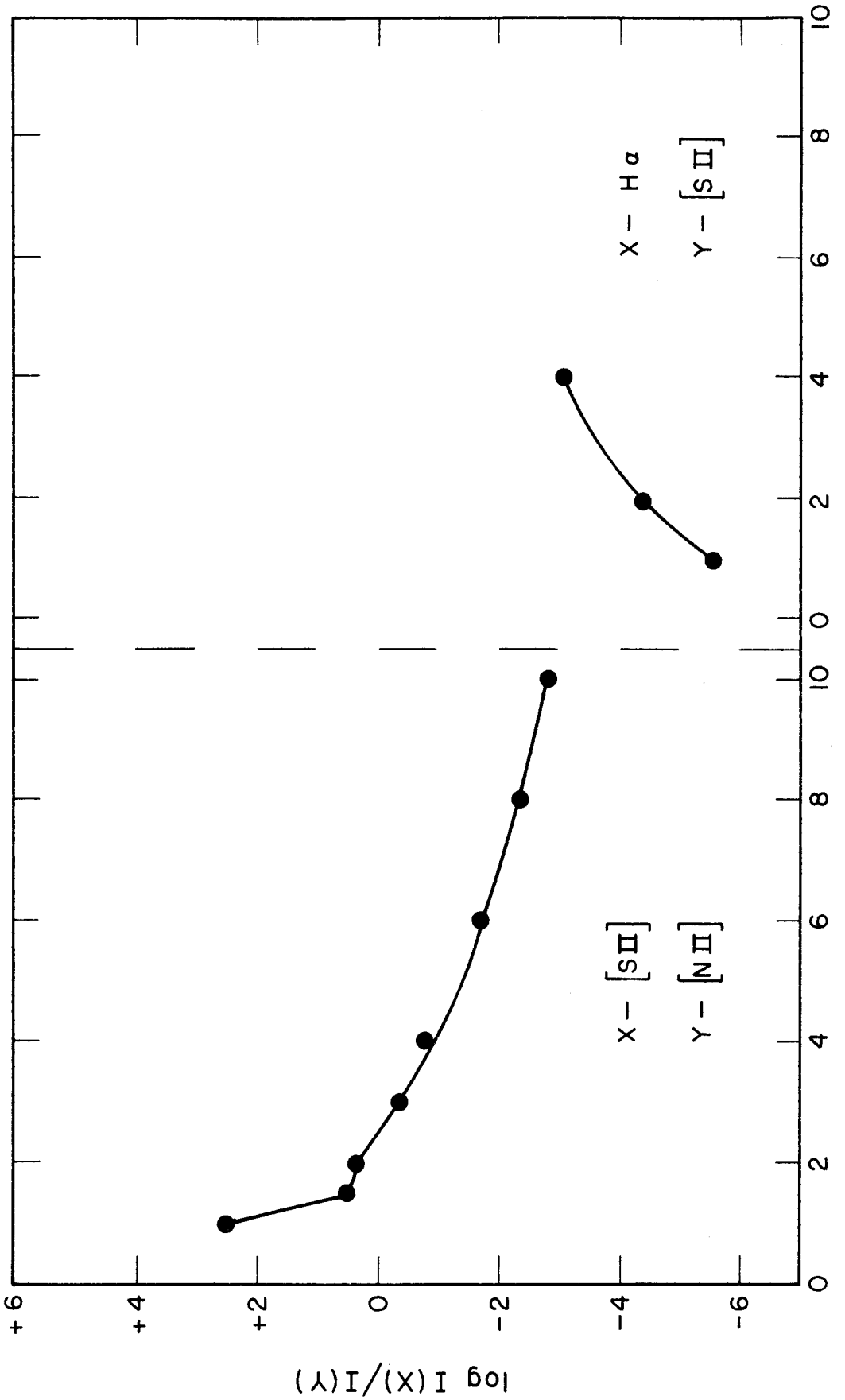

Figure 9

Figure 10

Relative intensities for equal numbers of atoms.

and the formulation of Osterbrock and Seaton. These ratios can be relatively sensitive functions of the density. Table 9 lists the results from the equation of Osterbrock and Seaton for the [OII] ratio. The values for the [OII] ratio obtained from the equation of Naqvi and Telwar varied in the same manner as those from Osterbrock and Seaton but were always slightly larger. The range corresponding to that shown in Table 9 was $1.19 < r < 1.48$. Table 18 of the Appendix lists the values for the [SII] ratio as derived from Naqvi and Telwar. For the densities considered here the ratio is insensitive to density variations.

In order to determine temperatures the best ratio would appear to be that between the [OII] doublet and the [OIII] doublet since it is so sensitive a function of temperature, and also since it is not dependent on abundances. For densities we will rely on the [OII] doublet ratio. With other ratios we will attempt to determine abundances. The ratio of [OII] and [NII] since it is sensitive to the effect of reddening and not a strong function of temperature can be used, once assumptions are made about abundances, to determine the reddening.

Basic to all work connecting the predicted ratios and the observed ratios is the assumption that the filaments are uniform in temperature and density, an assumption which almost certainly does not hold all the time but which if we remain well aware of it when the results are discussed we can allow to stand, at least for the Hydrogen atoms and the OII, NII, and SII ions among which stratification effects should not be too important.

TABLE 9

4([OII]) = I(3729)/I(3726)

N_e / T_e								
cm^{-3} \ °K	10^4	1.5×10^4	2×10^4	3×10^4	4×10^4	6×10^4	8×10^4	10^5
80	1.40	1.40	1.40	1.40	1.40	1.40	1.40	1.40
100	1.38	1.38	1.38	1.38	1.38	1.39	1.39	1.39
120	1.36	1.36	1.37	1.37	1.37	1.37	1.38	1.38
140	1.34	1.35	1.35	1.35	1.36	1.36	1.37	1.37
160	1.32	1.33	1.34	1.34	1.35	1.35	1.36	1.36
180	1.30	1.32	1.32	1.33	1.34	1.34	1.35	1.36
200	1.29	1.30	1.31	1.32	1.32	1.33	1.34	1.35
220	1.27	1.29	1.29	1.31	1.31	1.33	1.33	1.34
240	1.26	1.27	1.28	1.29	1.30	1.32	1.33	1.33
260	1.24	1.26	1.27	1.28	1.29	1.31	1.32	1.33
280	1.23	1.25	1.26	1.27	1.28	1.30	1.31	1.32
300	1.21	1.23	1.24	1.26	1.27	1.29	1.30	1.31
350	1.18	1.20	1.22	1.23	1.25	1.27	1.28	1.29
400	1.15	1.17	1.19	1.21	1.22	1.25	1.26	1.27
450	1.12	1.15	1.16	1.19	1.20	1.23	1.24	1.26
500	1.09	1.12	1.14	1.16	1.18	1.21	1.23	1.24
550	1.07	1.10	1.12	1.14	1.16	1.19	1.21	1.23
600	1.04	1.08	1.10	1.12	1.14	1.17	1.19	1.21
700	1.00	1.04	1.06	1.09	1.11	1.14	1.16	1.18
800	0.96	1.00	1.02	1.05	1.08	1.11	1.14	1.15
900	0.93	0.97	0.99	1.02	1.05	1.08	1.11	1.13
1000	0.90	0.94	0.96	0.99	1.02	1.06	1.08	1.11

CONCLUSIONS

The discussion following is based on the calculations presented above. The main justification for the use of these calculations which are for a collisional model is that as will be shown during the discussion, the Balmer decrement that is observed is that predicted by the collisional model and not that predicted for the case of radiative excitation and ionization. Further justification for this approach is found in the result, also to be discussed later, that for the Cygnus Loop indications are that virtually all of the observed radio emission can be explained in terms of free-free emission, so that there will exist no important high energy tail of synchrotron emission that could be the source of ionizing radiation. An independent way to check the importance of the ultraviolet continuum would be to determine the intensity of the continuum in the accessible regions and extrapolate this to the far ultraviolet. We observe that at $\lambda 3730$ the intensity of the continuum, which is never seen for certain, is less than 1% of that of H_α. Woltjer (1958) indicates for the Crab Nebula an extrapolation from the visual to the far ultraviolet at 300 A by decreasing the intensity per c/s by a factor of 10^2. From the appearance of the radio spectrum of the Cygnus Loop and from our ideas about the effects of aging on the spectra (Harris 1961) we would expect that the high energy cutoff for the synchrotron radiation of the Cygnus Loop will occur at a lower energy than for the case of the Crab. For this reason we could expect for the Loop a larger decrease in the intensity between the visual and the far ultraviolet. If we accept temporarily the figure of 10^2 and assign a thermal width of 4×10^{11} c/s to H_α, then we

find the intensity of the continuum at 300 A as $I(H_\alpha)/(4 \times 10^{11} \times 10^2 \times 10^2)$ or $3 \times 10^{-16} I(H_\alpha)$. Since the frequency at 300 A is 10^{16} c/s, and since the continuum is falling off very rapidly at this point, it seems possible to account in this fashion for a few times the energy radiated in H_α. The requirements, however, for many times the intensity of H_α probably at least 20 $I(H_\alpha)$ are definitely not met. The figures for the continuum intensity are, it must also be remembered, very much upper limits since the rate of fall off of the continuum intensity from the visual to the far ultraviolet is probably larger than the figure used and the figure for the continuum in the visual is only an upper limit. Besides most of the continuum intensity in the visual can probably be accounted for as free-free emission.

In the sections below, after accepting the validity of using the collisional model for the reasons expressed above, we shall first discuss in general the matter of the means of determining the temperature and then the indicated results for each object separately before summarizing.

Temperature Determination

A means exists of checking the applicability of the [OII]/[OIII] temperature to the regions in which the radiation of the other atoms and ions arises. The ratio, [SII]/[NII], is a function of the temperature and certainly not as liable to show the effects of stratification as the [OII]/[OIII] ratio. If the values of the two ratios are plotted for each point in the Cygnus Loop and IC 443 and if the [OIII] radiation pertains to the same temperature as the [NII], [OII], and [SII] radiation then

we will expect a correlation for all the points. If on the other hand the [OIII] temperature is completely unrelated to the temperature pertinent to the other forbidden lines we will find no correlation. In figure 11 the points are plotted as described and very apparently there is not correlation. The only possible explanation for this besides the meaninglessness of the [OII]/[OIII] temperature, would be that the abundances varied erratically from filament to filament. This situation is not indicated in the next figure in which we plot the values of the [SII]/[NII] ratio against the H_β/[OII] ratio. Figure 12 shows a strong correlation between the points and thus indicates that the temperatures indicated by the two ratios are related. It should be noted, however, that we cannot rule out completely the possibility that the changes in the ratios are not the result of small abundance changes that are correlated so that as the abundance of Sulphur increases relative to that of Nitrogen, the abundance of Oxygen decreases relative to that of Hydrogen.

To proceed further and find the temperatures indicated by these ratios we must first make assumptions about abundances. As stressed earlier about all we can strictly assume to know about the abundances of the elements in these nebulae is that they must be at least approximately equal to the normal interstellar or B star abundances. They can be over- but not underabundant relative to the norm. In this way for Oxygen and Nitrogen we will establish upper limits for the temperature. For the [SII] lines we consider the atomic constants so much more uncertain that we tend to give the Sulphur abundances little weight.

In this light we also find another very strong and independent reason for suspecting the temperature indicated by the [OII]/[OIII] ratio.

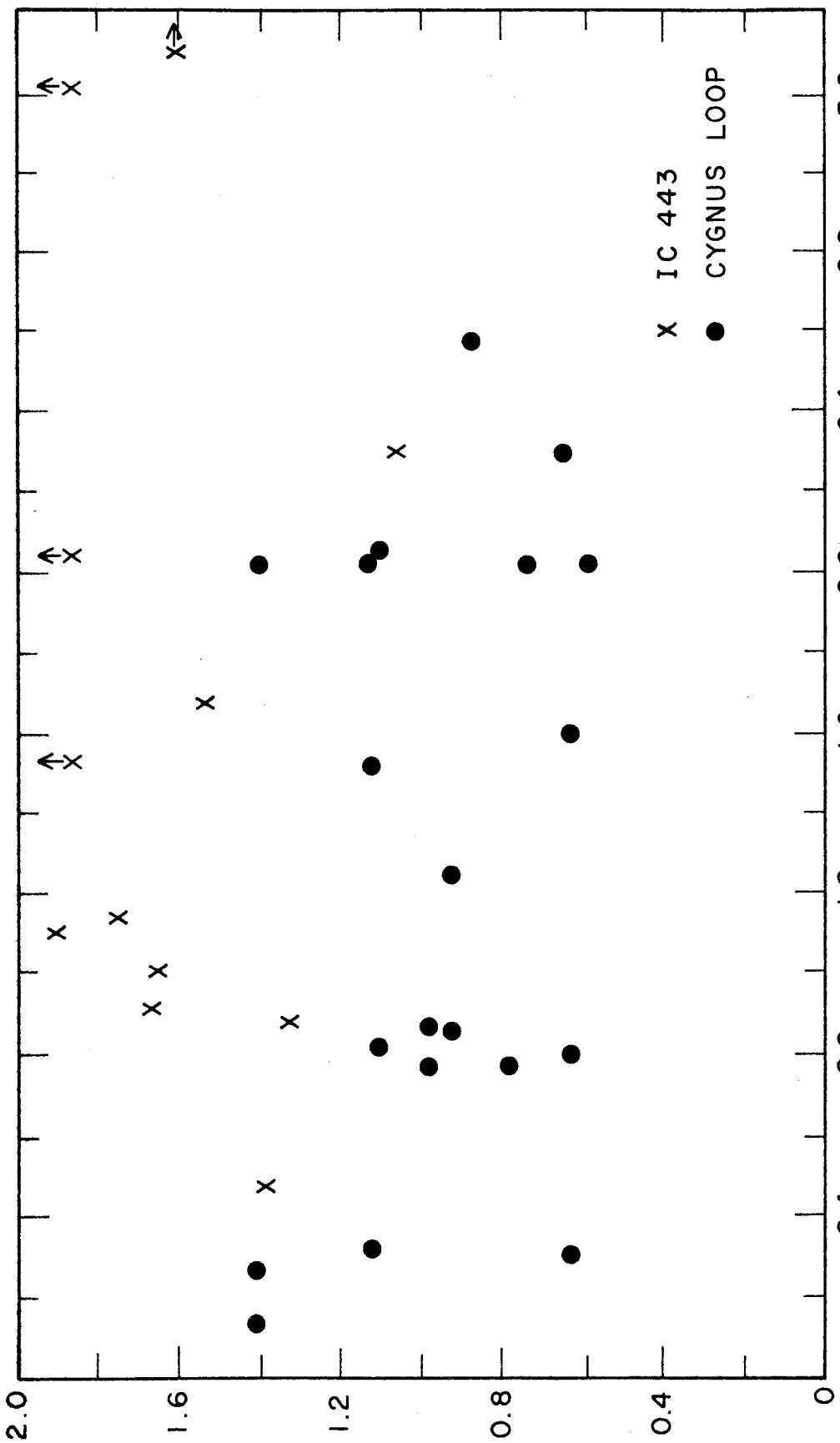

Figure 11: Correlation between I[SII]/I[NII] and I[OII]/I[OIII] for the Cygnus Loop and IC 443.

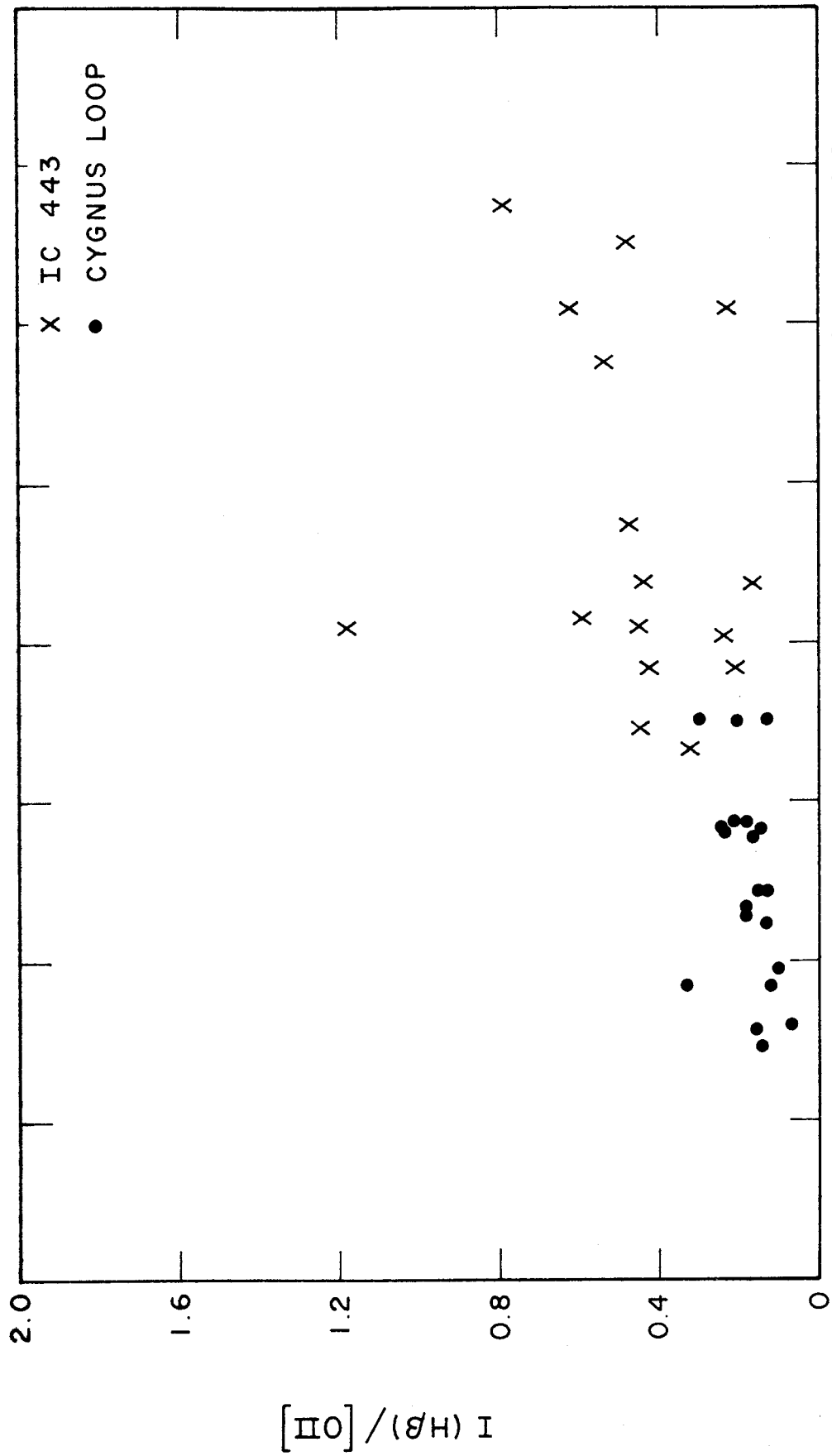

Figure 12: Correlation between $I(H_\beta)/I[OII]$ and $I[SII]/I[NII]$ for the Cygnus Loop and IC 443.

The temperatures so indicated run for instance in the vicinity of 40,000 ^{o}K for the Cygnus Loop and on the basis of, for example, the observed H_{β} [OII] ratio lead to a large underabundance of Oxygen which is unacceptable. In the following discussions we will have to consider the abundances indicated by the observations for the various values of the temperature and then try to obtain a temperature that seems to be least objectionable in the abundances it predicts.

The significance of the meaninglessness of the [OII]/[OIII] ratio can be understood in terms of the stratification mentioned earlier. In a model of the collisional mechanism using shock waves we have as discussed for instance by Sargent (1959) a situation in which there is at the front immediately behind the shock, an extremely hot rarefied region followed by a denser region of appreciably cooler temperature. Such a situation has also been previously discussed in connection with the emission line spectrum of the radio source Cas A. We thus require that the [OIII] radiation come from the hotter region and that there therefore exists no correlation between the [OII]/ [OIII] ratio and the temperature in either the hotter or cooler region. It goes without saying that we are, of course, not actually dealing with a two level situation but since the lines we are concerned with will tend to appear from two different temperature regions we can treat it as a two level case. Concerning the [OIII] emission it should be further pointed out that it is not clear from the observations whether the OIII is physically separated from the cooler region as in the shock model or whether it exists as OIII that has not had time to recombine as suggested by Minkowski and Aller (1954) for Cas A. Apparently at the densities involved here the

lifetime for this condition could be quite sufficiently long, greater than several thousand years.

Cygnus Loop

To illustrate the abundances and try to determine the temperature, we can, if we take a single temperature for the lines other than the [OIII] lines, indicate the different values obtained for a filament section. We shall pick on NGC 6960-4'(2) and -7'(2). In Table 10 we compare the three cases indicated by the different values of the temperature for the ions other than OIII. The "normal" values listed in the table are obtained from Aller (1961).

A solution of 10^4 °K, although it gives the best abundances for Oxygen tends to indicate a rather large overabundance of Nitrogen. Two statements should be made with regard to this situation. First, as indicated in figures 6 and 7 on pages 65 and 66 the temperature can be raised to 1.2×10^4 °K without affecting the Oxygen nearly as strongly as the Nitrogen so that a solution at this temperature would perhaps be more to our liking. Second, there is no strong reason why we should reject the overabundance of Nitrogen. Indeed Woltjer (1958) in his study of the Crab Nebula finds a rather similar result and the individual B star abundances do go as high as 43/100,000 for Nitrogen relative to Hydrogen. The Sulphur abundances we tend to treat lightly because of the poor knowledge of the Atomic parameters. The influence of possible errors in the determination of the reddening on the value of the temperature is relatively small. An increase of the reddening correction by a factor two would lead to a temperature increase of 3,000 °K.

TABLE 10

ABUNDANCES (NUMBERS OF ATOMS)

	H	N	O	S	
Planetary Nebulae	100,000	24	59	5	
B Stars (Range)	100,000	6-43	34-140	2-6	"Normal"
(Average)	100,000	15	59	3	
					T_e
NGC 6960-4'(2)	100,000	14	5	70	40,000
	100,000	10	17	3.6	20,000
	100,000	90	77	0.24	10,000
NGC 6960-7'(2)	100,000	18	4	105	40,000
	100,000	13	13	5	20,000
	100,000	115	61	0.4	10,000
NGC 6888-1'(6)	100,000	26	0.4	-	40,000
	100,000	18	1.4	-	20,000
	100,000	165	6.5	-	10,000
NGC 6888-2'(2)	100,000	7.5	0.2	-	40,000
	100,000	5.3	0.6	-	20,000
	100,000	48	2.7	-	10,000
			plates scanner		
IC 443-6"(1)	100,000	10	1 3	115	40,000
	100,000	7	4 10	6	20,000
	100,000	65	18 47	0.4	10,000
IC 443-6'(4)	100,000	8	1 2	132	40,000
	100,000	6	3 8	7	20,000
	100,000	54	13 35	0.45	10,000

Probably the most important ratio as far as this study is concerned is the ratio of H_α to H_β, which will indicate the mode of exciation prevalent in these objects. Comparison of Table 3, page 36 with Table 8, page 64, where the value of the Balmer decrement is listed for both radiative and collisional excitation in a gas optically thick to Lyman radiation shows that in all except four cases the indicated Balmer decrement is in reasonable agreement with the calculated decrement for 10^4 °K, and certainly not indicative of radiative excitation. Three of the exceptions to this observation are in filament 8, and it should also be pointed out that for these three cases the intensity of H_β is very much less than that of λ5007 with which it is directly compared and a relatively small uncertainty could affect the intensity of H_β by a very great amount; so these values should probably not be taken too seriously at this time. It may also be noted that the values of the Balmer decrement listed for filament 6 are perhaps inordinately high. For reasons discussed it seems plausible that this can be written off as due to a poor measure with the scanner.

The calculated Balmer decrement is rather insensitive to changes in the temperature so that we would have to modify the temperature very significantly and in the direction of cooling the nebula in order to indicate a trend toward radiative excitation. The reddening would have to be increased by a factor between 4 and 5 to adjust the observed decrement so that it would agree with the decrement calculated for radiative excitation in a medium that was optically thick to the Lyman radiation. To adjust the observed decrement so that it agreed with that calculated

for collisional excitation in a medium optically thin to Lyman radiation would require an increase in the reddening by a factor of 3 over that observed. Since the systematic errors in determining the reddening that such adjustments imply seem inadmissably large we must accept the conclusion that the situation with which we are dealing is one of collisional excitation of the Hydrogen spectrum in a medium that is optically thick to the Lyman lines.

Using a temperature of about 10^4 ^oK and the observed values for the [OII] doublet ratio we can from Table 9, page 69, determine the electron density which accordingly runs from 80 to perhaps as high as 600 electrons per cm^3. These values are not very sensitive to changes in the temperature.

Concerning the radial velocity picture of the Cygnus Loop, we can add nothing to the extensive work previously published by Minkowski (1958). The dependence of measured radial velocity on radial distance from the center of our measures is illustrated in figure 13. The curves are those of the model proposed by Minkowski (1958). The scatter of our points and their fit to the curves is quite comparable to that shown by Minkowski in the same region. Our lack of direct evidence either for or against the model is due to our lack of points closer to the center which in turn results from the fact that the primary purpose of our plates is not to measure radial velocities but to obtain spectrophotometric measures, so that we choose brighter and sharper filaments which occur for the most part along the rim.

In Table 5, page 51, we have listed the measured total flux in H_α from the various objects and also corrected these values for absorption

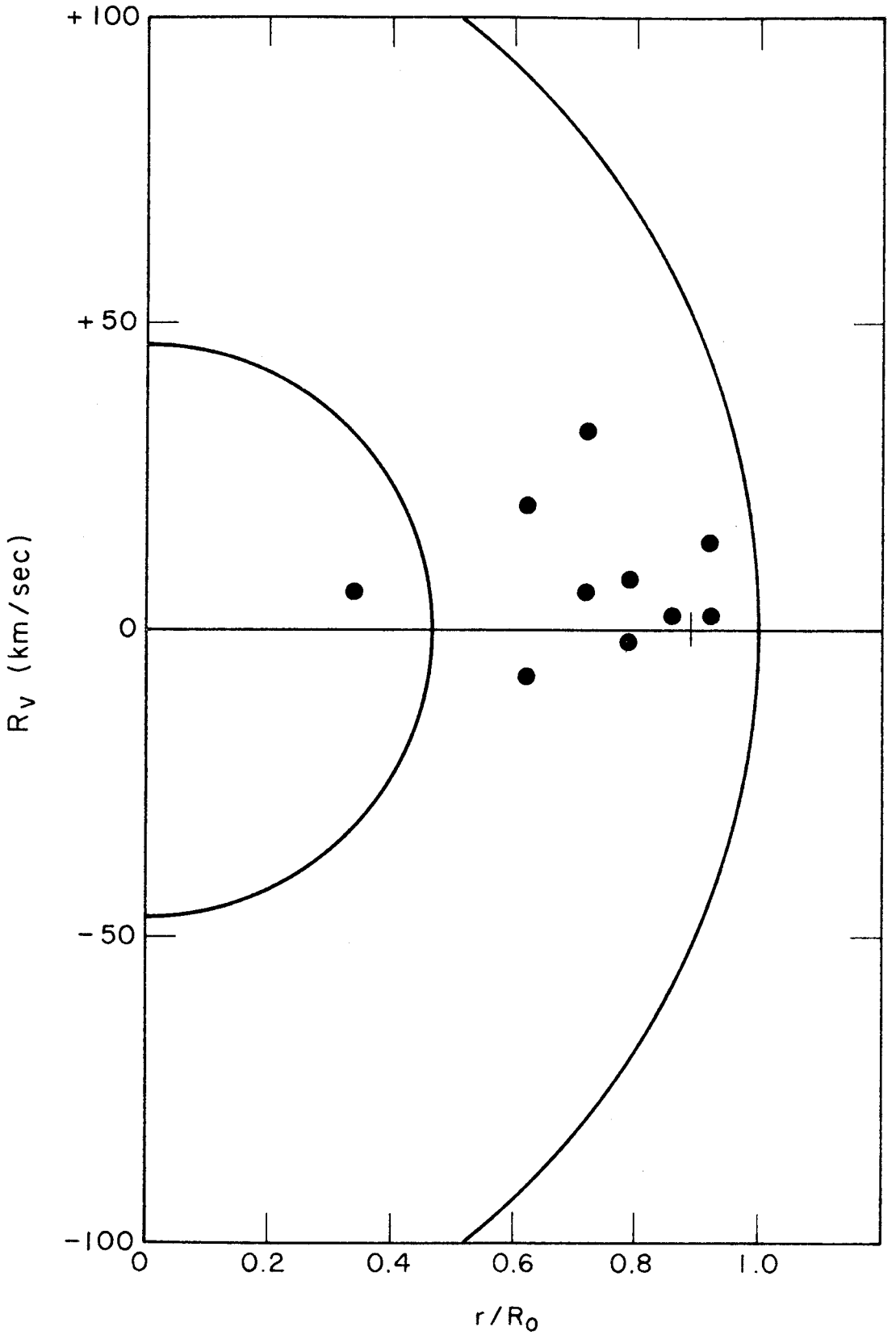

Figure 13: Radial velocity as a function of projected distance from the center of the Cygnus Loop.

as discussed above. For the Cygnus Loop we have measured only the flux from NGC 6992 and 6995. In the calculations that follow we can, where desirable, obtain the total flux of the whole loop by observing that the integrated part represents between one half and one third of the total, and since the calculations will be of a rather rough nature anyway we will not be led too far astray. The first comparison of interest would be to compare the observed radio emission with that which we can expect as free-free i.e. thermal emission, on the basis of the observed H_α radiation. From Oster (1961) we can expect that the intensity of free-free emission at 1000 megacycles will be given by the expression

$$I_{1000} = 4.8 \times 10^{-37} N_e N_i T_e^{-1/2} \text{ ergs/cm}^3\text{/sec/(c/s)}$$

Osterbrock and Stockhausen (1961) have demonstrated the validity of this equation for diffuse nebulae by measuring both the total H_β flux and the total radio flux at 22 and 30 cm from NGC 281 and showing that the H_β flux predicted by the use of the previous equation agrees with that observed to within the probable errors.

We also have the values given earlier in Table 17 of the Appendix for $I(H_\alpha)$ as a function of N_e and T_e. After adopting N_i as equal to $1.1\ N_p$ (Mathis 1957) it is clear that we need only specify the temperature in order to predict the amount of free-free radio radiation at 1000 megacycles from the observed amount of H_α radiation. If we take T_e as being about $1.0 \times 10^4\ ^\circ K$ then we find that

$$I_{1000} = 4.8 \times 10^{-39} N_e N_i$$

and

$$I(H_\alpha) = 0.23 \times 10^{-25} N_e N_p$$

and therefore

$$I_{1000} = 0.23 \times 10^{-12} I(H_\alpha)$$

which leads to a value of 1.4×10^{-21} ergs/cm^2/sec/(c/s) as the expected free-free radiation at 1000 megacycles from NGC 6992 and 6995. NGC 6992 and 6995 are coincident with Source C of the Loop as described by Harris (1961) for which he obtains a measured value of 2.6×10^{-22} ergs/cm^2/sec/(c/s) at 1000 megacycles so that we have accounted for five times as much radiation as is observed. Due to the sensitivity of the ratio between I_{1000} and $I(H_\alpha)$ to temperature, this prediction of more radio radiation that is observed is not bothersome and can be easily changed by raising the temperature. In fact if the temperature is raised to 20,000 $^\circ$K the 500% figure will be turned into a 6% figure. The figures at 10,000 $^\circ$K represent a great change from the calculations of Harris (1961) who used Chamberlain's (1953b) figures for $I(H_\alpha)$ and a temperature of 40,000 $^\circ$K. Indeed these results confirm to a large extent the expectation of Mathewson et al. (1961) who considered the spectrum of the Cygnus Loop to be a combination of a thermal (90%) component and a non-thermal (10%) component, on the basis of its having a rather flat spectrum. Because of our lack of an independent temperature we are prevented from saying more, but it appears that in the temperature range from 10 to 15,000 $^\circ$K we are capable of supplying all the free-free radio emission needed from NGC 6992 and 6995. Indeed since on the basis of the Balmer

decrement and the rather flat thermal appearance of the radio spectrum we might expect most of the radio emission to be free-free emission, we could attempt to fix the temperature by requiring that the predicted and observed radio fluxes agree.

The problem of Harris' source A which contributes six times as much radio radiation as source C with a spectral index very similar to that of C and yet is in a region quite devoid of filaments near its center may also be solved by assigning even lower temperatures to the few filaments in the central area. However, it would be desirable to have some independent spectroscopic evidence concerning the temperature in this area. It should be noted that because of the faintness of the filaments near the center of source A no spectra were obtained in the center of that region. However, filament 2 is located in the area of the source though not at the center, and we have also been able to examine two plates by Minkowski which are closer to the center, but none of these plates reveals any peculiarity as far as line ratios are concerned.

Finally if we have free-free emission in the radio region we can also inquire what intensity we would expect for a continuum in the optical region. For the case of free-free emission in a situation in which we have a Maxwellian velocity distribution Allen (1955) indicates that the energy radiated per c/s is proportional to $\exp(-h\nu/kT)$. The $\exp(-h\nu/kT)$ indicates that we would expect for a temperature of approximately $12,000\ ^{o}K$ that the optical continuum should be about 1/2 as intense per c/s as that in the radio region. The upper limit which we set as 1% of $I(H_{\alpha})$ is just 1/2 of the observed intensity of the radio continuum.

If we now take the distance to the Cygnus Loop as 770 parsecs we can compute the total mass on the basis of a uniform temperature of 10^4 °K, and an average density of 220 electrons per cm^3. The total radiation loss of NGC 6992 and 6995 in H_α is under these circumstances 4.2×10^{35} ergs/sec, as corrected for space absorption. From Table 17 of the Appendix we find that the rate of H_α emission at the density and temperature specified is

$$0.51 \times 10^{-23} N_P \text{ ergs/sec}$$

and thus we find the number of protons to be

$$N_P = 8.3 \times 10^{58}$$

so that the mass of Hydrogen is about

$$1.38 \times 10^{35} \text{ gm}$$

which when we correct for a ten percent Helium abundance yields a total mass for NGC 6992 and 6995 of 90 solar masses. The total mass for the Loop would then be between two and three hundred solar masses when we consider the visible filaments. As with the predicted values of the radio flux these figures for the mass are rather sensitive to the temperature and so, if the temperature is raised to say 14,000 °K so that the predicted and observed radio fluxes coincide, then the observed mass of the entire Loop will fall to between 40 and 60 solar masses. If, following this argument, we take the visible mass to be approximately 50 solar masses and if we now consider that all this mass is moving with a velocity of 100 km/sec then the kinetic energy of the filaments is 5×10^{48} ergs. If we further assume on the basis that the filaments are

optically thick to Lyman radiation that the amount of radiation in Lyman Alpha is ten times that in H_α, we will come to a figure of perhaps 2×10^{37} ergs/sec for the total loss through radiation of the whole Loop which leads to a value of the lifetime of the order of 2×10^{11} seconds, or several thousand years. It is of interest to note that for a mass of 50 solar masses moving at 100 km/sec we are concerned with a momentum that is quite in line with a mass of one solar mass being ejected by a supernova at a velocity of 5000 km/sec.

IC 443

The determination of the reddening in front of IC 443 through the use of abundances and line ratios is of course made more difficult since we are left without a method to determine temperature critically. An attempt was made to find a correlation between the values of the [SII]/[NII] ratio and the [OII]/[NII] ratio for each filament of the Loop. No such correlation could be found however, as indicated by figure 14. Thus we were forced to take an average value, 1.3, of the [OII]/[NII] ratio for the Cygnus Loop which we could then require all filaments in IC 443 to have when unreddened. This will then not allow any variation in the ratio of the [OII] and [NII] lines such as exhibited in the Loop. At any rate figure 8 shows that the ratio is not a very strong function of temperature and in fact reaches a rather flat minimum at 2×10^{4} °K. Forcing the [OII]/[NII] ratios in IC 443 to be equal to 1.3 we get a series of reddening values which are listed in Table 19 of the Appendix. Here R_1 is the reddening factor between the red and ultraviolet lines and R_2 is the reddening factor between the red and

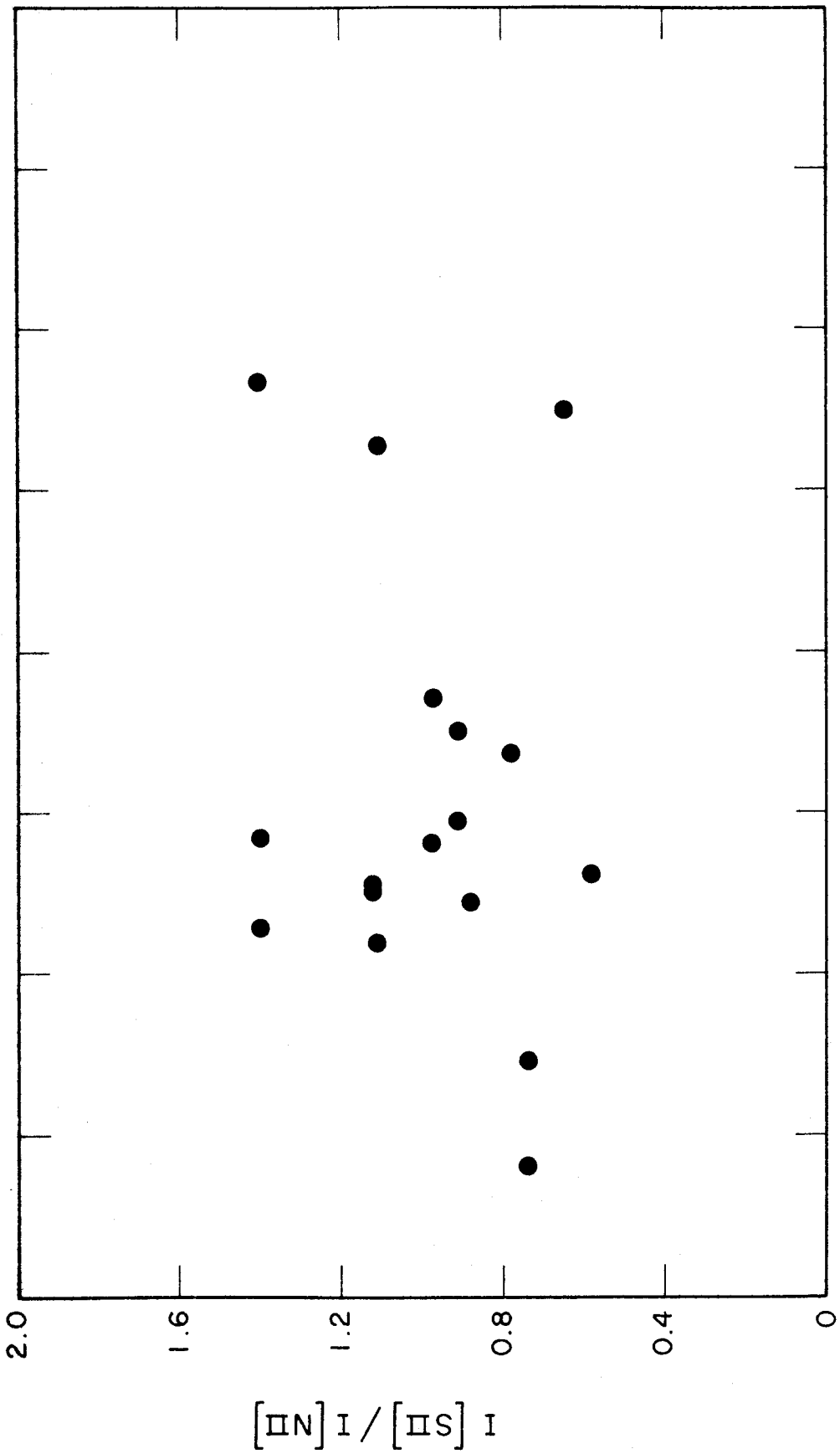

Figure 14: Correlation between I[SII]/I[NII] and I[OII] /I[NII] for the Cygnus Loop.

green or green and ultraviolet lines. $(R_2)^2 = R_1$. The average values for the whole object are 4.4 and 2.1 which corresponds to a value of $\rho\ell$ of 5.3 which does not disagree with the values derived from Hiltner (1956). This is the value of the reddening that we have used to correct the ratios of the lines as listed at the botton of Table 3, page 36.

Following the procedure of determining the temperature by comparing the abundances indicated by various values of the temperature we list in Table 10, page 77, the abundances as determined for three values of the temperature. Again we are forced by the Oxygen abundance to take a temperature close to 10^4 ^oK and in so doing accept an overabundance of Nitrogen. Accepting 10-15,000 ^oK as an approximate temperature we can now indicate that the density would appear to be of the order of 350 electrons/cm^3, slightly higher than in the Loop.

As far as the Balmer decrement is concerned a glance at Table 3, page 36, will reveal that the figures are no where near as uniform and satisfactory for the collisional case as in the Loop. It should be pointed out however, that the results are to a certain extent ambiguous because of the fact that for some of the sections that have been scanned, we have two values of the decrement arising from two different values of the $H_\beta/\lambda 5007$ ratio. This situation is indicated by the inclusion of two sets of figures for the H_α/H_β ratio for the affected sections in Table 3, page 36. Of course, the ambiguity can be demonstrated for only the filaments sections that were observed with the scanner. For the other sections of the filaments we can quote only one value; however, if the second value for the section of filament observed with the scanner is

correct, the Balmer decrement for the other sections of the filament would also be changed accordingly. Thus for IC 443-6'(4) the scanner measures indicate λ5007 to be twice as intense as H_β, while the spectrograms indicate the two to be roughly equal. The same situation also exists for IC 443-6" and IC 443-15'. In the same way it should be remembered that the tie in between the two sets of scanner observations, as indicated in Table 2, page 29, is rather poor for IC 443-7', 15', and 16'. The best that can be said here is that the results are inconclusive, Regarding abundances we have forced the Oxygen/Nitrogen ratio to be the same as that in the Loop and thus, because of our treatment of the Loop, forced it to be more or less "normal."

The H_α/[NII] ratio for IC 443 tends to be somewhat higher than for the Cygnus Loop. Therefore if we insist on exactly the same temperature for the two objects we will find the abundances a bit lower in IC 443 compared to the Loop. Alternatively we can take these ratios as indications of a lower temperature for IC 443. The [SII]/[NII] ratio which is higher in IC 443 than in the Loop also indicates that either the abundances have changed or the temperature is lower in IC 443. Thus although we cannot absolutely fix the temperature for either object we can say that <u>if</u> the abundances remain equal between the two, then IC 443 is cooler than the Cygnus Loop. Note however, that we are not in a position to completely rule out the possibility that there is an abundance change between the two such that in IC 443 Nitrogen is less abundant relative to both Hydrogen and Sulphur and Sulphur is more abundant with respect to Hydrogen, although this seems to be more unlikely than the possibility that the temperature is merely lower in IC 443. These

conclusions with regard to temperature are virtually independent of both systematic errors affecting the computations for all the ions and also, due to the location of the lines, errors in the reddening.

The results of the radial velocity measures are plotted as a function of distance from the apparent center in figure 15. Again the curves represent Minkowski's model for the Cygnus Loop. And, again little can be said as far as deriving a velocity picture of expansion. It should be noted that, on the basis of these measures, filaments 15' and 16' are both on the other side of the object. No meaningful distance can be derived using these radial velocity measures and the new proper motion measures. We can note however, that if IC 443 is expanding at the same radial velocity as the Loop the new proper motion measures will bring it in part way to about 1.5 kpc.

Working now with the total observed flux in H_a from IC 443 corrected for absorption, we can again calculate the amount of free-free emission at 1000 megacycles expected on the basis of a temperature of 10^4 °K and the H_a intensity as listed in Table 17, page 111. This time the calculated value is 3.0×10^{-21} ergs/cm^2/sec/(c/s) for the whole of IC 443 and amounts to about 150% of the total observed radio radiation at 1000 megacycles. The spectral index for IC 443 is listed in the radio region of -0.37 by Harris (1961) and so it is certainly more non-thermal in appearance than the Cygnus Loop. For IC 443 radio resolution is not as good as with the Loop because of its smaller size and so we are not able to say whether or not the smaller excess of predicted over observed radio emission for IC 443 in general is due to the fact that a lower tem-

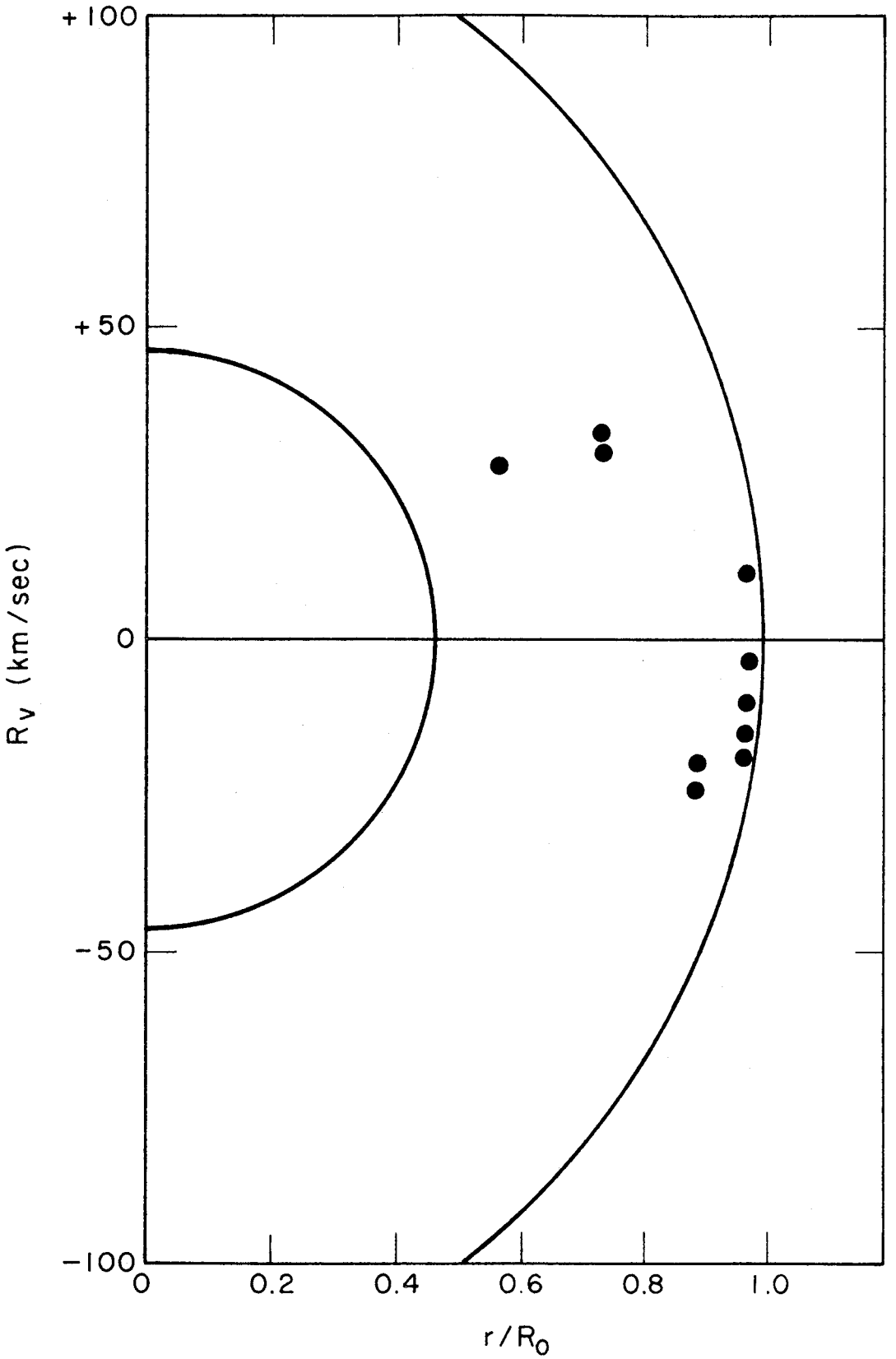

Figure 15: Radial velocity as a function of projected distance from the center of IC 443.

perature is pertinent to IC 443 compared to the Cygnus Loop, or due to the fact that indeed the non-thermal component of the radio emission is larger for IC 443 in general, or finally due to the fact that we have included, by integrating the whole object, a region in IC 443 that is similar to source A in the Loop. If on the same basis we were to carry out our calculations of the expected free-free emission for the whole Cygnus Loop we would also find a figure of between 100 and 200% of the observed value. In fact, however, the observations of the spatial distribution of the radio emission from the Loop show this to be somewhat irrelevant.

Before we can proceed to calculate the total flux emitted by IC 443 in H_α and thus its mass, we must say something about its distance. We are still not in a good position to determine its distance by comparing the radial velocity and proper motion of expansion. On the basis of the fact that it is about 1/3 the size of the Cygnus Loop and its proper motion of expansion is 1/3 to 1/2 of that of the Loop, it has been suggested that it is farther away from the Loop -- perhaps at 2 kpc. This idea is indeed not disputed by the reddening measured with the [OII]/[NII] ratio which indicates that the reddening agrees with that of stars at about the same distance. On the other hand Harris (1961) has suggested on the basis of filament sizes that it is located at approximately the same distance as the Loop. In the discussion below we shall use both distances with the idea that the real distance probably lies somewhere between the two.

The total flux in H_α from IC 443 is 5×10^{36} ergs/sec if it is

2 kpc away, or 8×10^{35} ergs/sec if it is only at a distance of 800 parsecs. Then assuming a temperature of 10^4 and a density of 350 electrons/cm^3 we find the total mass of the visible filaments to be 700 solar masses if it is at a distance of 2 kpc and 120 if it is at 800 parsecs. As before we can, of course, decrease this mass somewhat by raising the temperature. It might be pointed out in this connection that we are better able to accept a higher mass for IC 443 compared to the Loop since it is much closer to the plane of the galaxy and is thus probably located in a region of higher interstellar gas density.

Assuming a general velocity of expansion of 100 km/sec we again get a lifetime of the order of several thousand years. In fact the only ways we can change the lifetime of these objects since we calculate the mass from the total observed loss are by raising the temperature which increases the "efficiency" of the Hydrogen atoms at radiating H_α and so decreases the mass indicated by the observed emission, or by changing the velocity of expansion, or by changing the ratio between the total radiation loss and the radiation loss in H_α, e.g. by making the filaments optically thin to Lyman radiation. Actually the Balmer decrement would be quite different in the latter case and at least for the Cygnus Loop would not be in agreement with that observed.

NGC 6888

For NGC 6888 there would seem to be real question whether or not we can properly apply our calculations based on a collisional model since it could possibly be a giant planetary associated with the Wolf Rayet star HD 192163. However, the Balmer decrements listed in Table 3,

page 36, as corrected for reddening show very strongly that the excitation is collisional if the reddening is correct. Table 10, page 77, indicates that for even the 10,000 ^{o}K solution there is a very large underabundance of Oxygen, by a factor of about ten, while Nitrogen is already overabundant at 10^4 ^{o}K.

Following our previous discussion of the Cygnus Loop and IC 443 we could obtain a "normal" Oxygen abundance from the observed intensities by lowering the temperature. Unfortunately no values of the collisional b_n's for Hydrogen are available in this region but it can be observed from figure 6, page 65, that the $H_\beta/[OII]$ relation is rising at 10,000 ^{o}K. One difficulty in this attack is that the $H_\alpha/[NII]$ relation is also rising at 10,000 ^{o}K and so cooling the nebula would further increase the abundance of Nitrogen beyond that obtained at 10,000 ^{o}K and will result in probably a sizeable overabundance of Nitrogen. Although there is a large difference in the $H_\alpha/[NII]$ ratio between the two sides of NGC 6888 it should be noted that this need not require large variations in abundances between the sides since, as illustrated in figure 7, page 66, the difference can easily be accounted for by a slightly higher temperature for NGC 6888-1'. The differences in the $H_\beta/[OII]$ ratio between sides also indicate that we might expect a slightly higher temperature for 6888-1'. However, as discussed earlier, it is not possible to exclude completely the possibility of abundance differences. The Sulphur abundances are, of course, indeterminate because the [SII] lines were never detected. However, we are not necessarily forced into quite the same situation that we have with Oxygen, since all we can say is that the combined intensity of the [SII] doublet is less than 0.4 times I (H_α), which produces a Sulphur abundance

at 10^4 ^oK of $\leq$ 1 atom per 10^6 Hydrogen atoms.

We could also influence the Oxygen abundance without disturbing the Nitrogen abundance by changing the reddening. To make the abundance normal however we would have to change the reddening by a factor of 10 which would seem quite large. The question can then also be asked as to what would be the other consequences of increasing the reddening. If we left the nebula at the same position in space it would drastically increase the reddening in front of the Cygnus association as measured by Miss Roman (1951) and Hiltner (1956) by unallowably large amounts. The same arguments would apply if we were to try to move it closer. We could try to move it back along the arm. To increase the reddening, however, would also shift the Balmer decrement from a collisional to a radiative form and perhaps beyond. At the distance of 1600 parsecs where we place it by considering it to be associated with the Wolf Rayet star and thus the Cygnus association, the diameter of the ring in the long dimension is approximately 8 parsecs, and the mass as can be derived on the collisional model for 10^4 ^oK is 160 solar masses dimensions which does not really fit a planetary. If we were to move the ring away and increase the reddening we would then increase its linear size and its mass while at the same time requiring it to obtain a radiative means of excitation; so this does not appear to be the solution. We are not tied to the Wolf Rayet star directly since the Balmer decrement with the reddening indicated for the Wolf Rayet star indicates a collisional source for the excitation, however, we do not seem to be in a position to move NGC 6888 greatly in order to change its reddening to bring the Oxygen

abundance back to normal. Assuming again that the [OII] radiation is primarily from a region of about 10^4 ^oK we find that the indicated density averages about 400 electrons/cm^3. One final point which may or may not be relevant to the abundance picture for Nitrogen is the fact that the Wolf Rayet star which may be associated with NGC 6888 happens to be a WN star.

Radial velocities do not indicate anything particularly extraordinary about NGC 6888. And so we are left very much up in the air with a solution that indicates a collisional source of excitation and an anomalous abundance of Oxygen.

S 147

For S 147 no quantitative solution has been carried out because of the poor tie in between the integrations and because only one filament was studied. It can be observed that the densities are more or less the same as for the other objects and that the spectrum appears very similar to that of IC 443. The radial velocity measures indicate a perhaps larger than average velocity especially considering the proximity of the filament to the edge, however, we are not in a position to determine what portion of the indicated velocity is due to motion of the object as a whole.

S 22

For S 22 no work up was done because of the lack of observations. Like S 147 the line intensities are presented mainly so that they will be available. Although with S 147 we would be inclined to say that it is a supernova remnant like the Cygnus Loop because of its size, with S 22

we are really not in a position to say anything. There are stars inside the bend of the elbow which could possibly be exciting stars but we cannot go further. One really interesting thing about this object is the spectrum with λ6584 and even λ6548 stronger than H_α. This is an extension of the situation that we met in NGC 6888-1' and certainly on a collisional model with presently accepted cross-sections requires an abundance anomaly.

SUMMARY

The dominance of collisional excitation in the Cygnus Loop has been demonstrated conclusively. For IC 443 we are left with inconclusive results. For NGC 6888 collisional excitation is indicated by our solution but because the distance to the object is unknown and because of the peculiar results that accompany this solution we must reserve final judgement.

It has also been demonstrated that large changes in the temperature such as would be associated with a shock wave are found within filaments. This conclusion is influenced in part by the requirement of normal abundances. Using the criterion that neither Oxygen nor Nitrogen can be underabundant, we have shown that the temperatures of the cooler regions from which we receive the Balmer lines and the [OII], [NII], and [SII] doublets will be in the vicinity of 10,000 to 15,000 ^{o}K for these objects. Certain systematic errors for which correction cannot be made may affect this conclusion. These errors involve the lack of knowledge about the atomic parameters involved in the calculations. All our calculations are dependent on the semi-empirical ionization equation which we have been forced to use by the lack of collisional ionization cross-sections. Errors arising from it could cause us to over or underestimate the relative population of a given stage of ionization and thus obtain an incorrect abundance. In the same manner errors in the atomic parameters particularly Ω_{12} and A_{21} could lead to an incorrect idea concerning the population of the first excited state and hence again lead us to the conclusion of a wrong abundance at a given temperature.

Since our temperatures have depended on abundances they too may be affected. This situation is not a characteristic of just the case in which we find ourselves; the temperature determined by either [OII]/[OIII] or I(λ4363)/I(λ5007 + λ4959) would also be subject to unknown systematic errors due to errors in the atomic parameters.

As an illustration of the situation and also as part of the discussion of the abundance picture that we obtain, we note that for a given temperature, in the range of temperatures and densities considered here, the population of the first excited state of the various ions is to a good approximation a linear function of (Ω_{12}/A_{21}). Thus if we were to increase the value of Ω_{12} or decrease the value of A_{21} for NII by a factor of 5 we would be able to obtain "normal" Nitrogen abundances at 10^4 °K along with normal Oxygen abundances. By doing the opposite to the atomic parameters for Oxygen we could obtain a normal Oxygen abundance at 20,000 °K.

Attention should also be paid to the problem of the observed values of the H_α/[NII] ratio. Although nominally figured at 3:1 for radiative HII regions quite often in even apparently radiative cases the ratio falls to as little as 1:5; see for instance Baade and Minkowski (1954) and Burbidge and Burbidge (1962). From the calculations presented for the collisional case and from the example for NGC 6888, discussed above, it is apparent that to a certain extent this variation can be explained as arising from temperature variations. With a "normal" Nitrogen abundance under a collisional model the minimum of the H_α/[NII] ratio is still only 1:1; see figure 7, page 66. Two

ways are then open to decrease the ratio. The first, which we have accepted in our earlier discussion in the conclusion, is to accept an overabundance of Nitrogen. Such an overabundance by a factor of five does not appear to be too objectionable in some ways. The scatter of the "normal" abundances as listed in Table 10, page 77, is practically this large. Then too in view of the steepness of the H_α/[NII] relation as a function of temperature, what may be involved is that previous nebular determinations may have given improper abundances due to small errors in the temperature. The second way to explain the anomalously low ratio would be to increase the relative population of the first excited state either by increasing Ω_{12} or by decreasing A_{21} by a factor of five.

Certain aspects of the temperature or abundance picture are not affected by these possible systematic errors. If abundances are indeed constant between IC 443 and the Cygnus Loop we can also find evidence that, beyond the large differences in temperature from one part of a filament to another, some filaments are on the whole cooler than others. Thus for instance comparing filaments in IC 443 and the Loop we find for some filaments in IC 443 that relative to an "average" filament in the Loop the [SII] lines are enhanced relative to H_α and that H_α is enhanced relative to the [NII] lines. Such differences also occur from one filament to another in the same object. It must be remembered, however, that we are in the position of not being able to rule out completely the possible influence of small abundance changes as discussed earlier.

The densities that have been determined are in the range of a few hundred electrons per cm^3 and are pertinent to the cooler regions. Indeed they are really averages over the regions of temperature from which we receive [OII] radiation. Since some data concerning the [OII] doublet ratio for these objects has been previously published (Osterbrock 1958) it would be of interest to compare our figures with those listed by Osterbrock. His point one is apparently our filament NGC 6960-4' and his point eight is apparently our filament IC 443-6'(4). For the first case he lists a ratio of 1.47 on the basis of one plate while we find a value of 1.25 ± 0.05 from two plates. For the second case Osterbrock lists 1.10 for two plates while we find 1.15 ± 0.03 for two plates. The agreement thus seems reasonable. The values of the density derived by Osterbrock are for a temperature of 40,000 ^{o}K for the Loop on the basis of the observed value of the [OII]/[OIII] ratio, the reality of which we have already discussed. However, since the [OII] doublet ratio is not too sensitive to changes in temperature the densities which he obtained are not too far from those indicated by our study.

It would also be of interest to recall that using these densities and assuming the filaments to be cylindrical Osterbrock derives a mass for the visible portion of the Cygnus Loop on the basis of filament sizes and numbers that is only on the order of 1/10 of a solar mass. Since we obtain indications of the same density, our estimate of the visible mass of the Loop as being of the order of perhaps a few tens of solar masses would seem to imply a greatly larger volume. Our larger mass can thus be taken as evidence for the existence of fragments of shells

which we see edge on as filaments; it seems unlikely that the number and size of the filaments could have been missed by a factor as large as 100. If the temperature were actually as low as 10^4 ^oK which on the basis of the spectra and predicted radio fluxes seems a little low, then the disparity between our mass and that obtained by Osterbrock could be explained by the fact that although $N_e = 250$, $N_H = 25,000$ since the Hydrogen is only 1% ionized at 10^4 ^oK. For temperatures of the order of 15,000 ^oK the effect is quite small. We can now repeat the arguments raised in the past for the existence of shells and not filaments -- that we would expect on at least some of the objects to see filaments across the middle as in the Crab and that we actually do observe faint diffuse regions of emission in the central areas of the objects.

Although the values of the Balmer decrement and the extrapolation of the far ultraviolet continuum from which we conclude that there is insufficient high energy emission to account for the observed energy loss for the Cygnus Loop are not subject to the systematic errors possibly affecting the temperature, the conclusion that all of the observed radio emission from NGC 6992 and 6995 can be accounted for as free-free emission and hence that non-thermal radio-emission is unimportant is terribly sensitive to the temperature. However, even if there were considerable non-thermal synchrotron emission present, depending on the location of the cutoff frequency synchrotron emission in the far ultraviolet could still be unimportant as indicated independently by our observations of the Balmer decrement.

Also affected sensitivly by any systematic errors concerning the temperature would be the calculations of the total mass and hence also

the lifetimes based on the available supply of kinetic energy. It may be noted however, that even at 20,000 ^{o}K the mass of the Cygnus Loop will be around a few solar masses.

Mention should be made of the values measured for the [SII] doublet ratio which should also give indications of the density. Off hand with the densities found by the [OII] doublet ratio we should expect a rather uniform set of values for the [SII] ratio since the densities all lie on the low density shoulder of the relation between the [SII] doublet ratio and the density. What is observed however is a certain amount of scatter and a general trend to indicate considerably higher densities than those indicated by the [OII] doublet. This might then be taken to confirm the shock wave model in which we would expect the Sulphur lines to originate in a cooler and therefore also denser region. Restraint must be exercised here however since there is very considerable scatter and we know already that the values of the atomic constants used for Sulphur are not the best and Naqvi and Telwar (1957) have also found this effect in other objects. It should be remembered also that the calculations of the density dependence of the [OII] ratio carried out with the formulae and atomic constants obtained from Naqvi and Telwar gave results differing from those of Osterbrock and Seaton (1957) using apparently improved atomic constants. All this is not to say that the observed effect is entirely spurious but perhaps we should get some better constants for Sulphur before drawing definite conclusions.

Toward solving the problems of the abundances and masses and perhaps also the question of whether the OIII region is physically separate from the cooler region, we can suggest two sets of observations.

First and foremost it is desirable to determine the temperature of the cooler region. For this purpose we can try to observe the red [OII] lines, the blue [SII] lines or the other [NII] line. For the Cygnus Loop or NGC 6888 at least some of these ought to be measurable for the brighter filaments. Secondly if, in the situation of the OIII not being separated from the cooler region but not having had sufficient time to recombine, the excitation temperature is still that of the cooler region then a measurement of the intensity of $\lambda 4363$ which should be possible in the right observatory locations might allow us to distinguish between the two cases regarding the physical location of the OIII.

REFERENCES

Allen, C. W. 1955, Astrophysical Quantities, University of London, London.

Aller, L. H. 1961, The Abundance of the Elements, Interscience Publishers, Inc., New York.

Baade, W., and Minkowski, R. 1954, Ap. J., 119, 206.

Balonowsky and Hase 1935, Pulkowa Bull., 14, 2.

Bowen, I. S. 1955, Ap. J., 121, 306.

Burbidge, E. M., and Burbidge, G. R. 1962, Ap. J., 135, 694.

Chamberlain, J. W. 1953a, Ap. J., 117, 387.

Chamberlain, J. W. 1953b, Ap. J., 117, 399.

Elwert, G. 1952, Z. Naturforschung, 7a, 432.

Garstang, R. H. 1952, Ap. J., 115, 506.

Harris, D. E. 1961, Ph. D. Thesis at the California Institute of Technology.

Hebb, M. H., and Menzel, D. H. 1940, Ap. J., 92, 408.

Hiltner, W. A. 1956, Ap. J., 124, 669.

Hubble, E. P. 1922, Ap. J., 56, 162.

Hubble, E. P. 1937, Carnegie Institution Yearbook, 36, 189.

Johnson, H. L., and Morgan, W. W. 1953, Ap. J., 117, 313.

Keenan, P. C., and Morgan, W. W. 1951, Astrophysics, McGraw-Hill Book Company, Inc., New York.

Mathewson, D. S., Large, M. I., and Haslam, C. G. T. 1961, M. N., 121, 543.

Mathis, J. S. 1957, Ap. J., 125, 328.

Miller, F. D. 1937, Harvard Ann., 105, 297.

Minkowski, R. 1942, Ap. J., 96, 306.

Minkowski, R., and Aller, L. H. 1954, Ap. J., 119, 232.

Minkowski, R. 1958, Rev. Mod. Phys., 30, 1048.

Miyamoto, S. 1956, Z. f. Astrophysik, 38, 245.

Moore, C. E. 1945, Contributions from the Princeton University Observatory, #20.

Moore, C. E. 1949, Circular of the National Bureau of Standard, #467.

Naqvi, A. M., and Telwar, S. P. 1957, M. N., 117, 463.

Oke, J. B. 1960, Ap. J., 131, 358.

Oke, J. B. 1961, Ap. J., 133, 90.

Oort, J. H. 1946, M. N., 106, 159.

Oster, L. 1961, Ap. J., 134, 1012.

Osterbrock, D. E. 1958, P. A. S. P., 70, 180.

Roman, N. 1951, Ap. J., 114, 492.

Sargent, W. L. W. 1959, Ph. D. Thesis at the University of Manchester.

Seaton, M. J. 1953, Proc. Roy. Soc. A, 218, 400.

Seaton, M. J. 1954, M. N., 114, 154.

Seaton, M. J. 1958, Rev. Mod. Phys., 30, 979.

Seaton, M. J. 1960, Reports on Progress in Physics, 23, 313.

Seaton, M. J. and Osterbrock, D. E. 1957, Ap. J., 125, 66.

Wildey, R. L. 1962, Ph. D. Thesis at the California Institute of Technology.

Wilson, O. C., Munch, G., Flather, E. M., and Coffeen, M. F. 1959, Ap. J. Supp., 4, 199.

Woltjer, L. 1958, B. A. N., 14, 39.

APPENDIX I

Tables

TABLE 11

I (1/λ) NORMALIZED ABSOLUTE ENERGY DISTRIBUTION

λ	HD 15318	HD 130109
6731	0.965	0.978
6716	0.969	0.977
6584	0.986	0.995
6562	1.000	1.000
6548	1.002	1.000
6364		1.024
6300		1.035
5007	1.000	1.000
4959	1.008	1.007
4861	1.030	1.015
3862	2.240	2.408
3727	1.000	1.000

TABLE 12

TYPICAL EMULSION CORRECTIONS

λ6731	λ6716	λ6583	λ6562	λ6548	λ6364	λ6300	Emulsion + Filter
1.51	1.41	1.08	1.00	0.98			103_aF + OG
1.44	1.35	1.02	1.00	0.98			103_aF + OG
1.50	1.40	1.04	1.00	0.98	0.87	0.93	103_aF + OG
		1.19	1.00	0.92			103_aE + OG

λ5007	λ4959	λ4861	
1.00	0.68	0.42	IIaObkd + W2A
1.00	0.72	0.46	IIaObkd + W2A
1.00	0.71	0.41	IIaObkd + W2A

λ3868	λ3729	λ3726	
1.04	1.00	1.00	IIaObkd + C 5970
1.06	1.00	1.00	IIaObkd + C 5970

These are examples of the average values. Each set of corrections listed here applies to a different set of plates taken at a different time. The observed intensities on the plates are multiplied by these values to yield the true relative intensities.

TABLE 13

ATOMIC PARAMETERS

	$\Omega_{(1,2)}$	$\Omega_{(1,3)}$	$\Omega_{(2,3)}$	$A_{21}(sec^{-1})$	A_{31}	A_{32}	ω_1	ω_2	ω_3
OII	1.28	0.58	2.12	7.71×10^{-5}	0.046	0.135	4	10	6
OIII	1.59	0.22	0.64	2.8×10^{-2}	0.23	1.6	9	5	1
NII	2.17	0.31	0.50	4.0×10^{-3}	0.034	1.08	9	5	1
SII	2.02	0.383	12.7	1.07×10^{-3}	0.26	0.44	4	10	6

TABLE 14

IONIZATION POTENTIALS (eV)

	XI	XII	XIII	XIV	XV	XVI
Hydrogen	13.54					
Nitrogen	14.49	29.49	47.24	77.45	97.86	
Oxygen	13.56	35.00	54.71	77.39	113.87	138.08
Sulphur	10.31	23.3	34.9	47.29	72.5	88.03

TABLE 15

COLLISIONAL b_n's FOR HYDROGEN FOR NEBULA OPTICALLY THICK IN THE LYMAN LINES

$T_e(^oK)$	10^4	2×10^4	4×10^4
b_3	1.50	3.47	4.00
b_4	1.22	2.32	2.60

TABLE 16

$A_{nm}(sec^{-1})$ TRANSITION PROBABILITIES FOR SPONTANEOUS EMISSION FOR THE [OII] AND [SII] DOUBLETS

	$D_{5/2}- S_{3/2}$	$D_{3/2}- S_{3/2}$
OII	3.78×10^{-5}	16.51×10^{-5}
SII	6.31×10^{-4}	17.36×10^{-4}

TABLE 17

$I(H_\alpha)$ (ergs/atom/sec)

$I = A \times 10^{-n}$

N_e cm^{-3} \ T_e °K	10^4 A	n	2×10^4 A	n	4×10^4 A	n
80	0.18	(23	0.11	(21	0.30	(22
100	0.23		0.14		0.38	
120	0.28		0.16		0.45	
140	0.32		0.19		0.53	
160	0.37		0.22		0.60	
180	0.42		0.25		0.68	
200	0.46		0.27		0.75	
220	0.51		0.30		0.83	
240	0.55		0.33		0.91	
260	0.60		0.36		0.98	
280	0.65		0.38		1.06	
300	0.69		0.41		1.13	
350	0.81		0.48		1.32	
400	0.92		0.55		1.51	
450	1.04		0.62		1.70	
500	1.16		0.68		1.89	
550	1.27		0.75		2.08	
600	1.39		0.82		2.26	
700	1.62		0.96		2.64	
800	1.85		1.09		3.02	
900	2.08		1.23		3.40	
1000	2.31	(23	1.37	(21	3.77	(22

TABLE 18

r ([SII]) = I (6716)/I (6731)

N_e cm^{-3} \ T_e °K	10^4	2×10^4	4×10^4	6×10^4	10^5
80	1.49	1.49	1.49	1.49	1.50
200	1.49	1.48	1.49	1.49	1.49
400	1.47	1.47	1.47	1.47	1.48
600	1.46	1.46	1.46	1.46	1.47
800	1.45	1.44	1.45	1.45	1.46
1000	1.44	1.43	1.43	1.44	1.45

TABLE 19

REDDENING FOR IC 443

Location	R_1	R_2
IC 443-6'(1)	2.3	1.5
(2)	3.8	1.95
(3)	5.0	2.2
(4)	3.8	1.95
IC 443-6"(1)	3.8	1.95
(2)	5.6	2.4
(3)	5.4	2.4
IC 443-7'(1)	3.6	1.9
(2)	2.9	1.7
(3)	3.0	1.7
IC 443-15'(1)	6.2	2.5
(2)	3.8	1.95
(3)	4.6	2.15
IC 443-16'(1)	~10	~3.2

$$\left[I([NII])/I([OII]) \right] \times \frac{1}{R_1} = \text{True Ratio}$$